Nonlinear optics and transformation of light in gases

V. G. Arkhipkin and A. K. Popov

L. V. Kirenskiĭ Institute of Physics, Siberian Branch of the Academy of Sciences of the USSR, Krasnoyarsk; Krasnoyarsk State University

Usp. Fiz. Nauk **153**, 423–468 (November 1987)

A review of current theoretical and experimental research in the field of nonlinear optical frequency mixing in gaseous media: The authors examine fundamental physical principles and features of nonlinear optics of gases and vapors of chemical compounds. The experimental methods employed are described. Major advances in the fields of optical frequency conversion to infrared, vacuum–ultraviolet, and soft x-ray spectral ranges; improvement in the detection of weak IR signals by conversion to the visible and near ultraviolet ranges; and wavefront conjugation are described. Practical applications of discussed methods are emphasized.

TABLE OF CONTENTS

1. INTRODUCTION

The development of effective frequency conversion methods for laser radiation is one of the major problems of laser physics. These methods are of great scientific and practical importance for attaining new spectral ranges of coherent radiation and improving the techniques of radiation detection, selective laser action, and control over the state and composition of various media, including the atmosphere. The extension of available spectral ranges of narrowband tunable radiation to x-ray, vacuum-ultraviolet (VUV), and IR regions is of special importance, as is the development of new methods for continuous wave frequency conversion and improvement of IR detector sensitivity and wavefront correction methods. In recent years gaseous nonlinear media (GNM)—gases, metallic and chemical compound vapors—have found more and more application: in this review we shall refer to all gaseous media as "gases". Their promise lies in their transparency over broad frequency ranges; high resistance to radiation damage and recovery from breakdown; and the possibility of continuously varying their composition, concentration, depth and aperture. Most importantly, they make it possible to attack certain problems that are difficult or altogther impossible to solve using nonlinear crystals.

In gases the concentration of active centers is lower (by 5–7 orders of magnitude) than in crystals and the order of nonlinearities is higher. Since the power of generated radiation varies as the square of these quantities GNM at first sight appear unpromising for practical applications. But focused research into nonlinear optical processes in gases has revealed the circumstances in which gases can be used to solve scientific and practical problems, yielding such interesting results as third harmonic generation (THG) in metallic vapors with conversion factor (CF) of the order of 10%;[1] generation of infrared (IR) radiation in the 1–20 μm frequency range by means of stimulated Raman scattering (SRS) in metallic vapors with quantum CF reaching 50%;[2] conversion of weak IR radiation into the near ultraviolet (UV) with quantum efficiency of the order of 60%;[3,4] IR

 0038-5670/87/110952-25$01.80

image conversion[5,6] and the simultaneous conversion of wide IR frequency ranges into the visible range;[7] efficient wavefront reversal (WR) of laser radiation;[8,9] generation of coherent vacuum-ultraviolet (VUV) and soft x-ray (SX) radiation up to $\lambda = 35.5$ nm;[10–15] direct conversion of IR radiation to VUV[16] using higher-order atomic nonlinearities; continuous frequency mixing.[12,17] Devices based on GNM are coming into use in IR[2,7] and VUV[18–24] spectroscopy of atomic and molecular media, plasma and chemical reaction products; in holography;[25] as inputs into excimer amplifiers for the generation of intense VUV radiation with good spatial and spectral characteristics;[13] and in other applications.

The early experiments devoted to resonance nonlinear optical processes in metallic vapors played an important role in the development of nonlinear optics in gaseous media.[26] They stimuated research into the possibilities of using GNM for frequency conversion of laser radiation (see, for instance, Ref. 27).

Nonlinear optics of gases and metallic vapors possesses several distinctive features. Nonlinear susceptibilities of atoms and molecules increase as the pumping frequency approaches single and multiphoton resonances, but a number of competing resonance nonlinear processes appear as well. When metallic atoms are used as a nonlinear medium, dedicated machines are required to obtain homogeneous vapors and vapor mixtures with gases. Refraction coefficients in gases are not anisotropic, so wave matching requires special techniques. Thus, optimally effective frequency conversion in gases depends on a particular set of these parameters.

This review is devoted to the physical principles, experimental techniques, advances, and applications of nonlinear optics in gaseous media.

2. PHYSICAL PRINCIPLES OF NONLINEAR OPTICS IN GASEOUS MEDIA

2.1. Nonlinear polarization as a source of radiation at new frequencies.

Polarization, that is the dipole moment at a given frequency per unit volume of the medium, is the source of optical radiation. In some circumstances (for example in a dispersionless medium) polarization per unit volume $\mathscr{P}$ can be represented in a power series of the electric field component

$$\begin{aligned}\mathscr{P} &= \varkappa^{(1)}E + \varkappa^{(2)}E^2 + \varkappa^{(3)}E^3 + \varkappa^{(4)}E^4 + \ldots \\ &= \mathscr{P}^{(1)} + \mathscr{P}^{(2)} + \mathscr{P}^{(3)} + \mathscr{P}^{(4)} + \ldots,\end{aligned} \tag{1}$$

where $\mathscr{P}^{(1)} = \varkappa^{(1)}E$ is the linear polarization of the medium; $\mathscr{P}^{(2)} + \mathscr{P}^{(3)} + \mathscr{P}^{(4)} + \cdots = \mathscr{P}_{\text{nl}}$ is the nonlinear polarization; $\mathscr{P}^{(n)}$ is the nth-order nonlinear polarization; $\varkappa^{(1)}$ characterizes the linear properties of the medium and $\varkappa^{(n)}$ ($n = 2, 3, 4, \cdots$) characterize the nonlinear properties.

Let us represent the radiation field as a superposition of monochromatic waves

$$E = \frac{1}{2}\sum_j \{A_j \exp[-i(\omega_j t - k_j z)] + A_j^* \exp[i(\omega_j t - k_j z)]\}; \tag{2}$$

where A_j, ω_j, and k_j are, respectively, the complex amplitude, frequency, and wavevector of the interacting waves; "*" indicates complex conjugation. It is easy to see, by substituting (2) into (1), that nonlinear polarization components (beginning with $\mathscr{P}^{(2)}$) can serve as sources of radiation at sum and difference frequencies, as well as harmonics of the incident field. The magnitude of each nonlinear polarization component is determined by the field intensity and the magnitude of $\varkappa^{(n)}$. For example, the cubic nonlinearity $\varkappa^{(3)}$ can generate propagation polarization waves at the following frequencies: the third harmonic $3\omega_j$, sum frequencies $\omega_i + \omega_p + \omega_k$, $2\omega_i + \omega_k$ ($i \neq k$), and difference frequencies $\omega_i \pm \omega_k - \omega_p$, $2\omega_i - \omega_k$ and the like.

Similarly, ninth-order polarization can yield oscillation at the frequency $8\omega_i + \omega_k$. If ω_j corresponds to a wavelength in the ultraviolet, where the air is still transparent ($\lambda \gtrsim 2000$ Å), then the ninth-order nonlinearity will generate radiation of $\lambda = (2000\text{ Å}/9) \approx 220$ Å, i.e., in the soft x-ray range. By tuning ω_k we can also tune the frequency of this SX radiation. Hence nonlinear optical phenomena in gases can be used to push the short wavelength limit of laser radiation into the soft x-ray region. This possibility opens up new horizons for both fundamental research and numerous applications, such as thermonuclear plasma diagnostics, computer microcircuit processing, and other microtechnologies for altering the physical and chemical properties of matter, etc.

Another important application of nonlinear optics in metallic vapor is the generation, as well as detection and imaging of IR radiation. Let frequency ω_2 correspond to IR radiation. Then by adding laser radiation at ω_1 and using third-order nonlinear processes the original IR radiation can be imaged in the visible. Since the original quantum $\hbar\omega_2$ is replaced by a more energetic quantum $\hbar(2\omega_1 + \omega_2)$, the weak IR signal is not only shifted into the visible, but enhanced by a factor of $(2\omega_1 + \omega_2)/\omega_2$. For far IR radiation this new signal can be several tens of times stronger. Also, media with cubic nonlinearities have a significant advantage in that the weak frequency-converted radiation is shifted in frequency from the strong pumping signal.

In a similar fashion, high-power visible and UV lasers can be used to generate intense tunable IR radiation at difference frequencies, as well as stimulated Raman scattering frequencies, for the purpose of resonance stimulation of absorbing molecules, for example in order to control chemical reactions, or conversely to generate IR radiation which is not absorbed by the atmosphere or by optical materials. The development of sources of tunable IR radiation opens new vistas not only in physics, but in chemistry, biology, medicine, astrophysics, remote environmental sensing, etc.

2.2. Features of nonlinear optics in gases

Unlike crystals, where frequency conversion usually employs polarization proportional to E^2, in gases the major role is played by higher order nonlinear effects.

Radiation intensity I_s generated by an nth-order nonlinearity is proportional to

$$I_s \sim |\varkappa^{(n)}A^n|^2 = |\varkappa^{(n)}|^2 I^n$$

and, therefore, strongly depends on the intensity I of the original radiation field, the magnitude of nonlinear susceptibility $\varkappa^{(n)}$, and the order of the process. It can be shown theoretically that in the nonresonance case $\varkappa^{(n)} \sim N/E_{\text{at}}^n$, where N is the atomic concentration and E_{at} is a quantity of the order of typical atomic internal fields. Usually this last quantity exceeds the field intensity of even focused, modera-

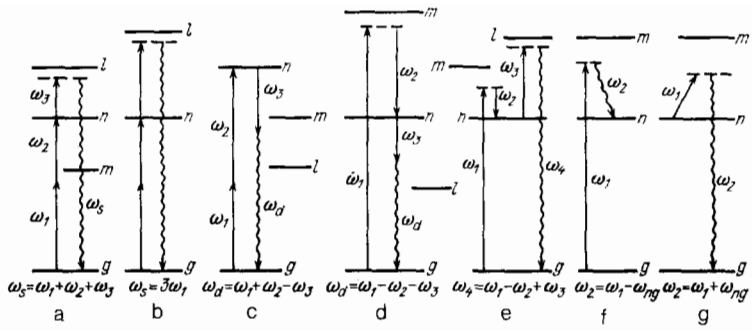

FIG. 1. Frequency conversion by a cubic nonlinearity via a two-photon resonance: a) Frequency addition; b) Third harmonic generation; c) Difference frequency generation; d) Difference frequency generation by SRS; e) Stimulated coherent anti-Stokes scattering; f) Stokes SRS; g) anti-Stokes SRS.

tely powerful laser radiation by two or more orders of magnitude. Taking into account that in gases the concentration is lower than in crystals by 5–7 orders magnitude, whereas the nonlinearity (n) is higher by at least an order, we can expect that generated power in gases, all other conditions being equal, should be lower by 14–18 orders of magnitude. That is why in the early years of nonlinear optics practical application of gases was considered impossible. This limitation, which appeared fundamental at first, has been overcome by employing resonance and quasiresonance nonlinear processes and determining the optimal frequency conversion conditions in view of the multitudes of physical processes that occur in intense laser radiation fields.

2.3. Resonance nonlinear susceptibility

It can be shown that for monochromatic waves in dispersive media the relation between the component of induced polarization at the sum frequency $\omega_s = \omega_1 + \omega_2 + \omega_3 \cdots + \omega_n$ and external fields can be written as

$$\mathcal{P}^{(n)}(\omega_s) = \frac{1}{2} P^{(n)}(\omega_s) \times \exp\{-i[\omega_s t - (k_1 + k_2 + \ldots + k_n) z]\} + \text{c.c.},$$

where the complex nth-order polarization $P^{(n)}(\omega_s)$ is defined by

$$P^{(n)}(\omega_s) = \frac{1}{2^{n-1}} \varkappa^{(n)}(-\omega_s, \omega_1, \omega_2, \ldots, \omega_n) A_1 A_2 \ldots A_n, \quad (3)$$

and $\varkappa^{(n)}(-\omega_s, \omega_1, \omega_2, \cdots, \omega_n) \equiv \varkappa^{(n)}(\omega_s)$ is the nth-order complex nonlinear macroscopic susceptibility. When treating frequency difference generation processes in equation (3) the sign of appropriate frequencies should be reversed and the amplitudes corresponding to these frequencies replaced by their complex conjugates.

In systems of free molecules or atoms, including gases, the macroscopic susceptibility $\varkappa^{(n)}$ is related to the microscopic (atomic and molecular) susceptibility $\chi^{(n)}$ and the particle concentration N by the simple product $\varkappa^{(n)}(\omega_s) = N\chi^{(n)}(\omega_s)$.

In isotropic media the lowest order of nonlinearity is $n = 3$. This nonresonance susceptibility $\varkappa^{(3)}$ is usually much smaller in gases than in liquids or solids. In gases nonlinear susceptibility can be computed from first principles: various approaches to calculating $\chi^{(3)}$ can be found, for instance, in Refs. 2, 28–33.

Consider how the resonance condition appears in nonlinear susceptibility. Examples of resonance nonlinear processes are illustrated in Fig. 1. The dominant term in the expression for $\chi^{(n)}(-\omega_s, \omega_1, \omega_2, \omega_3)$ (see Fig. 1a) is proportional to the factor (see, for example, Refs. 2, 28)

$$\chi^{(3)}(\omega_s) \sim \frac{d_{gm} d_{mn} d_{nl} d_{lg}}{\hbar^3 (\omega_1 - \omega_{mg})(\omega_1 + \omega_2 - \omega_{ng})(\omega_1 + \omega_2 + \omega_3 - \omega_{lg})}, \quad (4)$$

where ω_{ig} are the atomic transition frequencies, $\omega_s = \omega_1 + \omega_2 + \omega_3$, and d_{ik} are the projections of the electric dipole transition moments onto the electric field vectors of the pumping fields. In the nonresonance case the difference frequencies that appear in the denominator are of the order of transition frequencies. Multiplying them by $\hbar$ one obtains the transition energies, dividing by d_{ik} one obtains values of the order of atomic potentials. This is the dependence of nonlinear susceptibility on atomic fields to which we alluded earlier. Now let the field frequencies and their combinations approach transition frequencies—the denominator tends to zero.

In the limit the difference frequencies should be replaced by the transition half-widths Γ_{ig} (see, for instance, Refs. 2, 28). The two-photon resonance usually exhibits the least absorption. The advisibility of employing this particular resonance for harmonic generation was apparently first noted by Afanas'ev and Manykin.[34] It follows that if we make use of one resonance we enhance the generation by a factor of ω_{ig}/Γ_{ig}. For stationary atoms with a narrow resonance this gain is $10^{15}/10^8 = 10^7$. If the atoms move, Doppler shifts, averaged over the atomic velocities, appear in the denominator: the gain is then 10^5. If several resonances, for example, two-photon and three-photon ones, are simultaneously satisfied, the total gain equals the product of analogous separate gains (corresponding to stationary atoms). Consequently, resonances compensate for the low concentration of atoms and molecules in gases and reduce the need for high pumping intensities.

The full expression for nonresonance susceptibility $\chi^{(3)}$ contains a number of terms analogous to (4).[28–31] In many cases, the simplest method of obtaining an expression for $\chi^{(3)}$ is to use pictorial diagrams (see, for instance, Refs. 2, 31).

In Table I we cite the nonlinear atomic susceptibilities $\chi^{(3)}$ of several metals at two-photon resonance. A comparison of these values with typical nonresonance susceptibilities of alkali metals ($\chi^{(3)} \sim 10^{-34}$–10^{-32} in CGS units)[35] and noble gases ($\chi^{(3)} \sim 10^{-39}$–10^{-36} in CGS units)[36] illustrates the resonance gain (Fig. 2).

The generation of radiation with quantum energies exceeding the ionization energy invariably brings the ionized continuum states into the process. The ionized continuum spectrum can determine both the central features of the con-

TABLE I. Resonance nonlinear susceptibilities $\chi^{(3)}(3\omega)$ (two-photon resonances).[11]

Material	Resonance levels and states	$\lvert\chi^{(3)}(3\omega)\rvert \times 10^{-30}$, CGS units
Cs	$6s9d\ (^2D_{3/2})$	3,0
Mg	$3d\ (^1D_2)$	0,0897
Sr	$5s5d\ (^1D_2)$	0,51
Zn	$4s5s\ (^1S_0)$	0,31

version and the contribution of associated processes which may limit the conversion efficiency. Such associated processes include single and multiphoton ionization from the ground or (and) excited states.

When the continuum is taken into account expression (4) for nonlinear susceptibility must include integration over the continuum states, i.e, terms like

$$\chi^{(3)}(\omega_s) \approx \frac{d_{gm}d_{mn}}{\hbar^2(\omega_1-\omega_{mg})(\omega_1+\omega_2-\omega_{ng})} \int_{\varepsilon_1}^{\infty} \frac{d_{n\varepsilon}d_{\varepsilon g}}{\varepsilon-\hbar\omega_s}\,d\varepsilon, \qquad (5)$$

where ε_i is the ionization energy; $\omega_s=\omega_1+\omega_2+\omega_3$; and the integral in (5) refers to its principal value.

We have described above only the main features of nonlinear optical polarizations in quasiresonance media. In fact, one must also take into account the degeneracy of energy levels and selection rules for fields of different polarizations (see, for example, Ref. 2). The expression for $\chi^{(3)}$ becomes significantly more complicated because of saturation processes, the population of intermediate levels, the Stark effect, departures from monochromaticity, and so forth (see, for example, Refs. 2, 28 and the appendix).

2.4. Wave matching

In coherent nonlinear processes, like the generation of sum and difference frequencies, large amplitudes of nonlinear polarizations furnish a necessary but not sufficient condition for effective frequency conversion. The generated radiation will build up as it propagates through the nonlinear medium only if the propagating nonlinear polarization wave and the radiation it generates are phase matched. Only then will wave interference not transfer energy back into the pumping fields and periodically dampen the generated radiation along the medium. For example, the wave matching condition (nonlinear polarization and radiation in phase throughout the medium) for plane waves in the $\omega_s=\omega_1+\omega_2+\omega_3$ process is: $\Delta k=\mathbf{k}_s-(\mathbf{k}_1+\mathbf{k}_2+\mathbf{k}_3)=0$, where $\mathbf{k}_j$ are the wave vectors in the nonlinear medium. If $\Delta\mathbf{k}\neq 0$ the generated wave builds up only along the coherence length $L_c=|\pi/\Delta k|$.

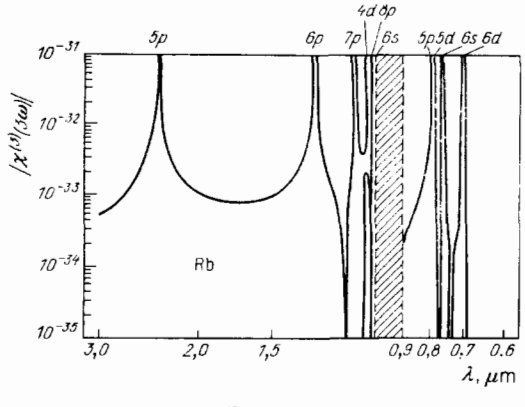

FIG. 2. Dependence of $|\chi^{(3)}(3\omega)|$ on pump wavelength in Rb atoms (CGS units).[35] In the striped region the approximation used to derive this curve is invalid.

In many cases, in order to achieve high pumping intensities the pumping field must be focused into the nonlinear medium. The pumping amplitudes are then large only in the focused spot, where most of the frequency conversion occurs. In the course of focusing, the spatial configuration of the nonlinear polarization and the radiation it generates must remain phase matched. In turn, given the pumping configuration, the spatial characteristics of nonlinear polarization are different for sum and frequency generation processes. The wave matching conditions are also different.[37] The amplitude of radiation focused at $z=f$ is conveniently represented by the Gaussian TEM_{00} mode

$$A_j = A_0(1+i\xi)^{-1}\exp[-k_j r^2 b^{-1}(1+i\xi)^{-1}], \qquad (6)$$

where $r^2=x^2+y^2$, $\xi=2(z-f)/b$, and b is the confocal parameter of the focused Gaussian beam. When $r=w=[b(1+\xi^2)/k_j]^{1/2}$ the field intensity is decreased by e compared to the beam center. The quantity w is sometimes referred to as the beam radius. At a distance $z=f\pm(b/2)$ from the focus the radius of the light spot increases by a factor of two over the radius at the focus. The full intensity in the beam is determined by the expression

$$W_j=\frac{c}{8\pi}\int_{-\infty}^{\infty}\int|A_j|^2\,dx\,dy=\frac{cA_0^2S}{8\pi}, \quad S=\frac{b\lambda}{4}, \qquad (7)$$

c is the speed of light.

The quantity S can be considered the effective area of the Gaussian beam at the focus. Neglecting pump depletion we can calculate the intensity CF for third-order processes in the field of a Gaussian beam as[37,38]

$$\begin{aligned}\eta_p&=\frac{W_4}{W_3}\\&=\nu_1\nu_2\nu_3\nu_4\left|\frac{16\pi^2}{c}\chi^{(3)}N\right|^2 F_j\left(\Delta kb;\frac{k''}{k'},\frac{b}{L},\frac{f}{L}\right)W_1W_2\\&=\nu_3\nu_4\left|\frac{4\pi^3}{c}\chi^{(3)}Nb\right|^2 F_j(\Delta kb;\frac{k''}{k'},\frac{b}{L},\frac{f}{L})\frac{W_1}{S_1}\frac{W_2}{S_2},\end{aligned} \qquad (8)$$

where $\nu_{1,2,3,4}$ are the wavenumbers ($\nu=\omega/2\pi c$); $k''=k_1+k_2+k_3$; $k'=k_1+k_2\pm k_3$ for sum ($j=1$) and difference ($j=2$) frequency generation processes respectively; $k'=k_1-k_2-k_3$ for $\nu_4=\nu_1-\nu_2-\nu_3$ ($j=3$); $\Delta k=k_4-k'$; and $k_{1,2,3,4}$ are the moduli of the radiation wave vectors. The function F_j is known as the dephasing (or phasing) integral, it is examined in detail by Bjorklund.[37] In general, in the case of a nonlinear medium of length L this function depends on the depth of focus with respect to the center of the medium (f/L), the amount of dephasing at b, and also on the type of the nonlinear process j.

An analysis of (8) demonstrates that in the case of strong focusing ($b\ll L$) at the center of the nonlinear medium, F_j is entirely determined by the magnitude of the parameter $b\Delta k$. But in general, the optimal values of this parameter vary with the medium density, with wave mismatch at fixed density (because of synchronizing impurities, for example),

and with confocal parameter. In particular, when $k''/k' \approx 1$ and Δk changes while the atomic concentration remains fixed, the peak conversion in Gaussian beams is attained at the following values of $b\Delta k$:

$$\begin{aligned}(b\Delta k)_{\text{opt}} &= -2, \quad \nu_4 = \nu_1 + \nu_2 + \nu_3,\\ &= 0, \quad \nu_4 = \nu_1 + \nu_2 - \nu_3,\\ &= 2, \quad \nu_4 = \nu_1 - \nu_2 - \nu_3.\end{aligned} \tag{9}$$

If the medium is made up of a single component and phase matching is achieved by changes in concentration, peak conversion is achieved at slightly different values of $b\Delta k$. In the $k''/k' \approx 1$ approximation the peak conversion parameters are

$$\begin{aligned}(b\Delta k) &= -4, \quad \nu_4 = \nu_1 + \nu_2 + \nu_3,\\ &= \mp 2, \quad \nu_4 = \nu_1 + \nu_2 - \nu_3,\\ &= 4, \quad \nu_4 = \nu_1 - \nu_2 - \nu_3.\end{aligned} \tag{10}$$

It therefore follows from (10) that, unlike their $j = 1,3$ counterparts, $j = 2$ processes can be efficient in media with both negative and positive dispersion. When $k''/k' \approx 1$ the optimal values $(b\Delta k)_{\text{opt}}$ depend on k''/k'—as this parameter increases the conversion efficiency falls off.[39]

In weakly focused Gaussian beams ($b \gg L$) phase matching is achieved by means of a wave mismatch (the opposite of plane waves):

$$\begin{aligned}(\Delta k)_{\text{opt}} = 2m_j b^{-1}, \quad m_j &\approx -2, && j = 1,\\ &\approx k''(k')^{-1} - 1, && j = 2,\\ &\approx k''(k')^{-1} + 1, && j = 3,\end{aligned} \tag{11}$$

which is necessary to compensate for the additional mismatch caused by the beam divergence. As $b \to \infty$ the optimal mismatch goes to zero, as it should for a plane wave.

2.5. Higher-order nonlinearities, direct and cascade processes

As we noted earlier, frequency addition and subtraction involving an odd number of photons higher than three is possible in an isotropic nonlinear medium. Such processes can be due to higher-order nonlinearities like $P^{(n)} = 2^{1-n}\chi^{(n)}NA^{(n)}$ ($n = 5, 7, 9, \cdots$) or to multistep conversion on lower-order nonlinearities. For instance, the fifth harmonic can be generated both by a fifth-order nonlinearity and by a third-order nonlinearity. In the latter case the third harmonic is generated first and then the third-order nonlinearity combines the third harmonic photon with two pump photons: $P^{(3)}(5\omega) = \chi^{(3)}NA(3\omega)A(\omega)A(\omega)/4$. The higher the order of the direct nonlinear process, the larger is the combination of lower-order cascade processes required to generate radiation at the same frequency. Consequently, in the general case one must consider the full conversion, which is determined by the interference of the direct and cascade interactions.[40] In a particular case, the contributions of the direct and cascade processes can be distinguished by considering the existence of intermediate q-photon resonances, the value of n, concentration N, and the type of focusing. This is true because the field intensities generated by each elementary process participating in a cascade depend on the above parameters. In general, wave matching conditions also depend on the type and order of process, and the degree of focusing.[41-43]

In direct nth order processes formula (8) can be generalized to[42]

$$W_s = \frac{\pi^4 2^{2(n+1)}}{c^{n-1}b^{n-3}} |N\chi^{(n)}|^2 \nu_s \times \prod_{p=1}^{n} \nu_p W_p F_j^{(n)}\left(\Delta kb; \frac{b}{L}, \frac{f}{L}, \frac{k''}{k'}\right). \tag{12}$$

$F_j^{(n)}$ (j describing the type of process) takes on its simplest form in the case of harmonic generation.[10,43] The form of $F_j^{(n)}$ for the general case is discussed in Ref. 42b (for $n = 5$ see Ref. 42a). As in the case of third-order processes, the optimal values of $(b\Delta k)_{\text{opt}}$ depend on the variation of other parameters; for instance, in sum frequency generation using strong focusing the optimal values are:

$$\begin{aligned}(b\Delta k)_{\text{opt}} &= -2(2n-2), && N \text{ changes},\\ &\quad -2(2n-4), && \Delta k \text{ changes}, N \text{ fixed},\\ &\quad -(n-1), && b \text{ changes}.\end{aligned} \tag{13}$$

When cascade processes are taken into account, the amplitude of generated radiation becomes a sum of terms due to direct and cascade processes as well as their interference. The expression for generated power becomes more complicated. Still, in a number of cases it can be represented by formula (12).[42] For example, in the case of weak focusing radiation generated by direct and cascade processes is characterized by the same wave mismatch. The quantity $\chi^{(n)}$ in (12) should simply be replaced by $\chi_{\text{eff}}^{(n)}$, which is the sum of the direct process susceptibility and the products of susceptibilities characterizing lower-order cascade processes weighted by coefficients which depend on N.

In the case of focused beams the expression for $F_j^{(n)}$ can also, in some circumstances, be reduced to (12). In particular, in fifth harmonic generation we should set $n = 5$ in (12) and replace $F_1^{(5)}$ by $|\mathcal{F}_1^{(5)} + \beta\mathcal{F}_1'|^2$, where $|\mathcal{F}_1^{(5)}|^2 = F_1^{(5)}$ and $|\mathcal{F}_1'|^2 = F_1$ are phase matching integrals for direct and cascade processes respectively, and β is the ratio of their contributions:

$$\beta = i6\pi\nu_1 bN\chi^{(3)}\chi^{(3)\prime}(\chi^{(5)})^{-1};$$

$\chi^{(5)}$ is the fifth-order atomic susceptibility for the direct process, $\chi^{(3)}$ is the third harmonic susceptibility, and $\chi^{(3)\prime}$ is the susceptibility for the sum frequency process $\nu_3 + \nu_1 + \nu_1$.

Quasiresonance nonlinear atomic susceptibility for the nth-order sum frequency generation $\omega_s = \omega_1 + \omega_2 + \cdots + \omega_n$ has the form (see Ref. 40):

$$\chi^{(n)}(\omega_s) = \hbar^{-n} d_{gm} d_{mn} \ldots d_{hg}\,[(\omega_1 - \omega_{mg})(\omega_1 + \omega_2 - \omega_{ng}) \ldots (\omega_s - \omega_{hg})]^{-1};$$

assuming that only the ground state g is populated. Experiments and theoretical estimates indicate that even at concentrations $N \approx 10^{16}$–10^{17} the macroscopic susceptibility $\varkappa^{(n)} = N\chi^{(n)}$ can equal or exceed nonlinear susceptibilities in crystals. Frequency conversion efficiency can also be much higher in gases, because gases have a much higher optical breakdown threshold (this permits markedly higher pumping intensities) and simplify phase matching. In Fig. 3

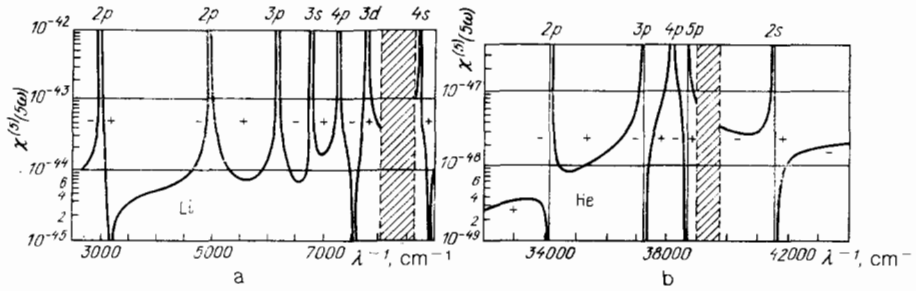

FIG. 3. Dependence of $\chi^{(5)}(5\omega)$ on pumping wavelength in a) Li, b) He.[42] " + " and " − " indicate the sign of nonlinear susceptibility in a given region.

we plot $\chi^{(5)}$ against wavelength for Li and He atoms.

In higher-order nonlinear processes several multiphoton resonances may be used simultaneously to further enhance nonlinear effects.

In order to increase higher-order nonlinear susceptibilities it may be expedient to use radiation collisions[2] with polarization exchange in two-component mixtures.[44]

2.6. Autoionization resonances

Autoionization (AI) states have a major effect on the nonlinear properties of atoms and simple molecules at VUV frequencies, as they produce resonances in certain regions of the continuous absorption spectra of many-electron atoms.[45] Al photoabsorption resonances typically have asymmetric profiles, with one wing exhibiting a minimum due to interference between direct ionization transitions and those to Al states followed by transitions to the continuum (Fig. 4). The presence of Al states not only alters the single-photon absorption cross section, but also the multiphoton ionization, cross sections and the nonlinear susceptibilities responsible, for example, for four wave mixing processes.[46,47]

When we take Al states into account formula (5) is modified to the following form[47]

$$|\chi^{(3)}|^2 = |\chi_0^{(3)}|^2\,[a^2+(x+q)^2]\;(1+x^2)^{-1}, \qquad (14)$$

where $\chi_0^{(3)}$ is the nonlinear susceptibility without the Al resonance and x is the relative detuning from the Al level. The generation profile is determined by the only two parameters, a and q, which depend on the properties of the atom. In the general case the profile is asymmetric (Fig. 5) with a maximum and a minimum; when $a = 0$ it reduces to the Fano Al resonance curve in photoabsorption. Four wave mixing using Al resonance was also investigated in Ref. 48.

Other studies[49] have shown that the resonance enhancement using Al states is usually effective in optically thin media, in which the absorption of generated radiation may be neglected. It is possible, however, that the generation profile differs significantly from the direct ground state photoabsorption curve, i.e., weak photoabsorption at the generated frequency may be associated with a relatively high value of $|\chi^{(3)}|^2$.

The Al resonance profile may change significantly when subjected to sufficiently strong fields.[47,50] This effect was first predicted by Geller and Popov,[51] who used the narrowing of Al resonance in the nonlinear susceptibility in a strong field as an example of how the position and width of such resonances may depend on the intensity of one of the pumping fields. In particular, in certain circumstances it is possible to narrow down the Al levels to their radiation width, which is ordinarily masked by configuration interaction broadening. These effects should be considered when Al resonances are studied by generation spectroscopy techniques; they make possible nonlinear spectroscopy inside the autoionization broadened profile. They can also be used to enhance nonlinear susceptibility in VUV generation at resonance with the Al level. Analogous effects have been predicted for photoabsorption and multiphoton ionization processes.[47] In recent years, due to advances in VUV generation techniques, the subject of Al resonances in strong laser fields has attracted greater and greater interest. Similar effects have been discussed in connection with predissociation in strong electromagnetic fields.[52]

2.7. Induced autoionization-like resonances

We have already noted the utility of Al processes for increasing nonlinear susceptibilities. It is often the case, however, that no Al resonances are available in the spectral

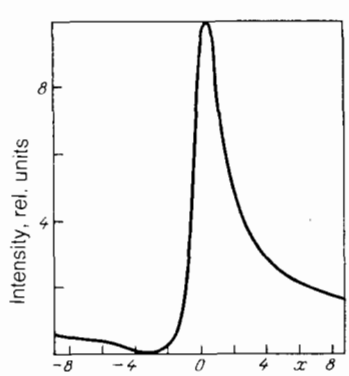

FIG. 4. Characteristic autoionization resonance profile in photoabsorption as a function of relative frequency separation x.[47]

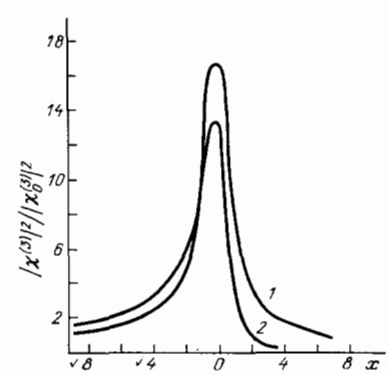

FIG. 5. Characteristic autoionization resonance profile in the nonlinear susceptibility.[47] 1: $a = 4$, $q = 2$; 2: $a = 2$, $q = -3$.

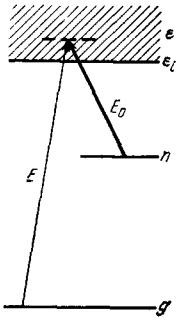

FIG. 6. Induced autoionization-like resonance diagram in photoabsorption and ionization.

range of interest. One then explores the possibility of inducing so-called autoionization-like resonances in arbitrary regions of the continuum by the use of an additional laser field E_0 that will stimulate transitions between an unpopulated excited discrete level and continuum states (Fig. 6).[47] This effect can be observed both in ionization and photoabsorption processes, and in the nonlinear susceptibility $\chi^{(3)}$ (Fig. 7).

In weak inducing fields the appearance of the induced resonance may be interpreted as due to higher order resonance nonlinear processes. These last can proceed via intermediate states both in the discrete and the continuum parts of the spectrum. Interference of these processes can lead to the appearance of a resonance in the continuum with the same properties as an autoionization resonance. In the case of strong inducing fields, when many orders of perturbation theory need generally be considered, nonlinear resonances in the continuum background are best interpreted as a consequence of strong electromagnetic field mixing of the discrete and continuum states that produces a discrete quasilevel.

Autoionization-like resonances lead to the same modifications in the expressions for nonlinear susceptibility, absorption and refraction coefficients, and ionization cross-sections as real Al states.[47] By changing the frequency and intensity of the inducing field we can vary the characteristics of the autoionization-like resonance. In the course of inducing Al-like resonances, the enhancement of frequency mixing susceptibility may, depending on the circumstances, be accompanied by decreased absorption of generated radiation and optical activity which makes it possible to control the angular and polarization characteristics of the photoelectrons (see Refs. 47, 53–56, and references therein).

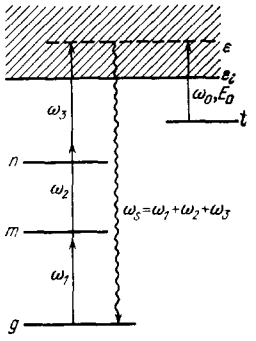

FIG. 7. Induced autoionization-like resonance diagram in nonlinear susceptibility.

2.8. Even order nonlinearities

Even order susceptibilities contain an odd number of matrix elements in the numerator and even number of frequency separations in the denominator. For example, in the $\omega_3 = \omega_1 + \omega_2$ process the quasiresonance susceptibility has the form

$$\chi^{(2)}(\omega_3) = \frac{d_{gm}d_{mn}d_{ng}}{\hbar^2(\omega_1 - \omega_{mg} - i\Gamma_{mg})(\omega_1 + \omega_2 - \omega_{ng} - i\Gamma_{ng})}, \quad (15)$$

In centrally symmetric media, like gases, in the absence of constant external fields electric transitions are allowed (i.e., d_{ik} differ from zero) only between levels of opposite parity. Therefore, in the electric dipole approximation, GNM that are unperturbed by strong external fields exhibit linear susceptibilities of odd order only—third, fifth, seventh, etc. In the dipole approximation there is no quadratic nonlinearity in isotropic media; hence the common notion that even order processes are ineffective and possible only in some special circumstances: such as constant external fields that destroy central symmetry (see, for example, Ref. 29) or the use of higher order multipoles—magnetic dipole and quadrupole transitions.[57,58]

In gases, second harmonic generation 2ω or the sum and difference frequency generation ($\omega_3 = \omega_1 \pm \omega_2$) using a static external field is determined by $\chi^{(3)}(-\omega_3;\omega_1, \pm\omega_2, 0)$. In this case conversion efficiency is usually low. Gauthier and co-workers have shown[59] that metallic vapors in an electric field can exhibit large nonlinearities when the resonance is tuned to the Rydberg transition frequencies. Then the required intensity of the external electric field becomes fairly small (1000 V/cm).

Even order susceptibilities may appear because of magnetic dipole and quadrupole transition moments when the propagation direction and polarization of the interacting fields is properly chosen[58] or an external magnetic field is applied.[60] Multipole transition moments are generally small compared to dipole ones. However, should one of the energy terms in the denominator of the nonlinear susceptibility corresponding to, say, one or two-photon quadrupole (magnetic dipole) transition, become small due to resonance,the nonlinear polarization may be markedly enhanced. In effect we must compensate a small numerator (a product of transition matrix elements) by a small denominator (small frequency detuning). In some cases the resulting nonlinear susceptibility proves sufficiently high to support frequency conversion of continuous wave laser radiation.[61]

A number of experiments involving strong pumping fields observed resonance generation of radiation on even order nonlinearities without external electric fields, even via transitions having neither a dipole, nor a magnetic dipole or quadrupole moments.[62–64] For example, Refs. 63, 64 reported not only second harmonic generation (with CF $\sim 10^{-1}$–10^{-2}), but also fourth (CF $\sim 10^{-6}$–10^{-8}), whereas Ref. 65 even reported eighth harmonic generation in Hg vapor. The conversion factors achieved on quadratic nonlinearities correspond to nonresonance four wave mixing. Possible mechanisms, including macroscopic currents and electron-ion separation in multiphoton ionization, generation of constant magnetic and electric fields by inhomogeneous pumping, and other mechanisms that destroy symmetry are discussed in Ref. 66.

2.9. Stimulated Raman scattering

Nonlinear optical polarizations at sum and difference frequencies are determined by products of complex amplitudes. Consequently their phase depends on all participating fields. Such processes are known as coherent or parametric. There are processes in which the nonlinear polarization is proportional to the squares of amplitude moduli. For example, the nonlinear process described by the cubic polarization

$$P^{(3)}(\omega_2)=\frac{1}{4}\chi_R^{(3)}(-\omega_2;\ \omega_1,\ -\omega_1,\ \omega_2)N|A_1|^2A_2, \quad (16)$$

corresponds to stimulated Raman scattering on the n–g transition. Here, for individual atoms and molecules

$$\chi_R^{(3)}(\omega_2)=\frac{|d_{gm}|^2|d_{mn}|^2}{\hbar^3[(\omega_1-\omega_{mg})^2+\Gamma_{mg}^2](\omega_1-\omega_2-\omega_{ng}+i\Gamma_{ng})}, \quad (17)$$

$P^{(3)}(\omega_2)$ does not depend on the phase of A_1 and has the frequency and phase of the field described by A_2. Such processes are known as incoherent. In coherent processes the initial and final states of the atoms coincide—only the photon distribution changes. In incoherent processes both the atomic and the photon systems change. For example, in (16) the atom moves from level g to level n, a $\hbar\omega_1$ photon disappears, while another $\hbar\omega_2$ photon is added to the system (see Fig. 1f).

If in the course of Raman scattering the atom or molecule moves to a higher-lying energy state, the result is Stokes scattering at a frequency lower than the pumping field. In the opposite case we have anti-Stokes scattering at a higher frequency (see Fig. 1g). Amplification at the anti-Stokes frequency requires that the upper energy level be more populated than the lower.

The intensity gain of a weak, monochromatic Stokes wave I_s in the field of intensity I_1 is described as follows (see, for example, Ref. 2):

$$I_s\sim\exp(Gz),\quad G=gI_1=-\frac{4\pi\omega_2 N}{c}\operatorname{Im}(\chi_R^{(3)}|A_1|^2). \quad (18)$$

For SRS on vibrational-rotational transitions the gain exponent G can be conveniently expressed using the differential cross-section of spontaneous RS,[2,67] as determined by experiment. SRS output power is determined by the distribution of spontaneous amplified sources, saturation proceses, etc. (see Ref. 2 and references therein). The threshold pumping intensity required to transform spontaneous scattering into SRS is usually estimated from the criterion $GL\geqslant 30$ (L is the length of the medium), when the intensity of scattered radiation becomes of the same order as the pumping intensity. In theory all pump photons may be converted to Stokes radiation, but competing processes limit realistic conversion factors.

In nonlinear optics of gases SRS processes on electron transitions (SERS) of metallic atoms are especially important. The optimal conditions for SERS are discussed in Ref. 2 and elsewhere. The threshold and spectrum of SRS usually depend on the pump spectrum (see, for example, Ref. 68). If the pump spectrum broadens, the threshold usually increases, but in resonance conditions ($\omega_1-\omega_{mg}\gg\Gamma_{mg}$) there exist configurations wherein the gain is described by (18) independently of the pump spectrum. The problem of resonance SERS with a nonmonochromatic pump field has not been examined in detail.

Pump focusing increases diffraction losses in the generated radiation when $\omega_2/\omega_1\ll 1$ (for alkali metals $\omega_2/\omega_1\sim 10^{-1}$–$10^{-3}$),[69] increasing the threshold and narrowing the generated frequency band. Additional stimulation of the n–g transition by a two-photon or biharmonic pump lowers the scattering threshold,[29] but then scattering is not purely Raman in origin.

SRS in gases can also occur on transitions that use up several pump photons (see, for example, Ref. 67). Such scattering is described by higher order nonlinear susceptibilities and is known as hyper-Raman scattering (HRS). The presence of radiation at frequency $\omega_2>\omega_{ng}$ can lead to higher order SRS ($\omega_3=\omega_2-\omega_{ng}=\omega_1-2\omega_{ng}$; $\omega_4=\omega_3-\omega_{ng}=\omega_1-3\omega_{ng}$ and so forth) and to generation of higher order anti-Stokes components.[70] Scattered radiation can participate in parametric interactions that result in coherent anti-Stokes scattering at $\omega_3=2\omega_1\pm\omega_2$ and $\omega_3=\omega_1-2\omega_2$ frequencies.[29,71] These are stimulated four-photon parametric threshold processes; as resonance is approached population inversion may occur in some transitions, leading to superluminescence which may play the role of the generating field.[2,71]

It should be noted that in some cases lacking population inversion the intensity of spontaneous anti-Stokes Raman scattering (SARS) may significantly exceed the luminescence of thermal sources.[72] If the pump frequency is tuned, the scattered frequency is also tuned. A number of papers have addressed the different methods of populating metastable atomic, molecular, and ionic levels, including autoionization levels, with the goal of obtaining spontaneous or, in some cases, stimulated SARS in the VUV and SX ranges.[72,73]

In gases incoherent nonlinear processes, like multiphoton absorption, are also being used to produce inversion and ordinary gain on allowed transitions in the VUV.[74]

In section 2 we have presented a simplified account of nonlinear processes in resonance gaseous media. In real life not all resonances are accessible because of strong absorption. In gases resonances are broadened by Doppler effects due to atomic motion and, in any case, the radiation itself has some finite spectral width. This reduces the resonance gain. As we have noted, competing nonlinear processes become significant at resonance in a strong laser field. Among other factors, the spatial homogeneity of the medium's optical properties is disturbed, imposing additional limitations. These problems are discussed in the literature, for example Refs. 2, 29, 33, 75–80, 219 (and in references therein)—they should be considered in each particular case in order to deduce optimal conversion conditions.

3. EXPERIMENTAL TECHNIQUES

We have already noted that certain values of phase mismatch ΔkL or Δkb are a necessary condition for effective frequency conversion in coherent processes, depending on the particular type of nonlinear process. At fixed concentration N, the magnitude and sign of the refraction coefficient at various frequencies and, consequently, the magnitude and sign of Δk can be controlled by tuning the pump or generated frequency near the single photon transition frequencies from populated states.[81] In particular, for plane wave pumping the optimal value $\Delta k=0$ is fulfilled by selecting the pump frequency such that $\omega_4\operatorname{Re}\{\chi^{(1)}(\omega_4)\}=\Sigma_q\omega_q\operatorname{Re}\{\chi^{(1)}(\omega_q)\}$.

Then Δk becomes independent of concentration and spatial inhomogeneities in the distribution of nonlinear atoms. This method, however, requires tunable pump lasers and can generate only certain frequencies in a given medium.

Another phase matching technique consists of adding an additional gaseous component to the nonlinear gaseous medium[82] This additional component mainly contributes with appropriate sign to the refraction coefficient at either pump or generated frequency. The necessary phase mismatch can be selected by changing the ratio of the nonlinear and synchronizing components. For example, the $\Delta k = 0$ condition can be achieved by the following ratio of component concentrations

$$\frac{N_c}{N} = \frac{\omega_4 \operatorname{Re} \chi^{(1)}(\omega_4) - \sum_q \omega_q \operatorname{Re} \chi^{(1)}(\omega_q)}{\sum_q \omega_q \operatorname{Re} \chi_c^{(1)}(\omega_q) - \omega_4 \operatorname{Re} \chi_c^{(1)}(\omega_4)}, \qquad (19)$$

where N_c and $\chi_c^{(1)}$ are, respectively, the concentration and atomic linear susceptibility of the synchronizing gas at the indicated frequencies. Consequently, nonlinear experimental technology using gaseous media typically includes various devices for mixing gaseous components.

At pump frequencies in the visible and near visible ranges metallic atoms exhibit the required two-photon resonances. Because of their chemical activity and high melting temperature glass and quartz ovens are ineffective. The preferred technology for obtaining metallic vapors of appropriate concentrations, as well as mixtures of such vapors with synchronizing buffer gases, employs single and concentric heat-pipe ovens.[83]

Figure 8 illustrates the main features of a single heat-pipe oven. A close-mesh induction coil is positioned along the inside walls of a stainless steel pipe. The metal to be vaporized is deposited on the coil. The central region of the pipe is heated by the heater, while the ends, capped with transparent windows, are cooled by running water. The pipe is filled with a buffer gas at a pressure approaching the desired vapor pressure. As the saturated metal vapor approaches the gas pressure, the heated region comes to be filled with mainly homogeneous metallic vapor, whereas the cold gas is found outside this region. Metallic vapors that diffuse to the cold regions condense and return to the heated region via the coil by capillary action. This cycle ensures fairly rapid heat exchange and large temperature gradients at the heated regions boundaries.

For phase synchronization one requires uniform temperature and some means of altering the concentration ratio of metallic vapor to synchronizing component in the heated region. The concentric heat-pipe oven serves the purpose (Fig. 9).

The concentric heat-pipe oven consists of two concentric pipes. By varying the gas pressure in the outside pipe it is possible to vary and stabilize the saturated vapor pressure and therefore the temperature of the heated region in the inner pipe. Moreover, the heated region has sharp boundaries at the ends and is homogeneous throughout. The heated region temperature determines the metallic vapor pressure in the inner pipe. The synchronizing gas pressure in the inner pipe can be independently varied over a relatively large range. Using this heat-pipe oven construction with a mixture of Rb and Xe Bloom and co-workers obtained CF of up to 10% in THG at $\lambda = 354.7$ nm.[1] The features of concentric atomic ovens were also discussed in Ref. 84.

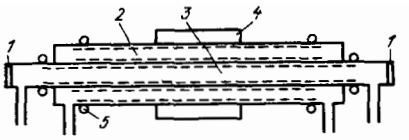

FIG. 9. Concentric heat-pipe oven for producing mixtures of metallic vapors and inert gases:[83] 1—windows; 2— metallic vapor; 3—metallic vapor mixed with synchronizing gas; 4—heater; 5—cooling chamber.

On occasion a different metallic vapor is used as the synchronizing component. The oven proposed in Ref. 85 and used by Bloom and co-workers[86] serves this purpose (Fig. 10). Its distinguishing feature is the absence of an induction coil from the central part of the heated region. As above, the temperature of the heated region (the synchronizing metal with the highest melting point is deposited in the inner region without the coil) is determined by the vapor pressure in the outer pipe. Thus, by varying the pressure in the outer pipe it is possible to vary the vapor pressure of the synchronizing component (Mg in Ref. 86). In turn, the vapor pressure of the nonlinear component (Na in Ref. 86) is set by the difference in the vapor pressures of the buffer gas in the inner pipe (with can be varied independently) and the synchronizing component. A disadvantage of this construction is that with time the synchronizing component tends to condense and solidify on the coil because of its higher pressure and melting point.

Heat-pipe ovens have the advantage that the windows remain cold and uncontaminated with metal; they can be made replaceable by means of the usual vacuum contacts. A modified heat-pipe oven with improved atomic density along the pipe axis was developed by Scheingraber and Vidal[87] (Fig. 11). A different construction[88] may be used for less refractory and chemically active metals (such as mercury) (Fig. 12): it is characterized by high vapor homogeneity and low absorption outside the nonlinear conversion region (focus region).

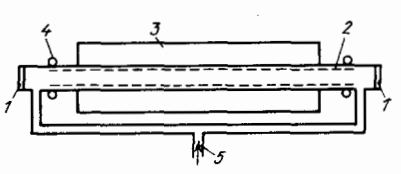

FIG. 8. Heat-pipe oven:[83] 1—windows; 2—induction coil; 3—heater; 4—cooling chamber; 5—gas intake.

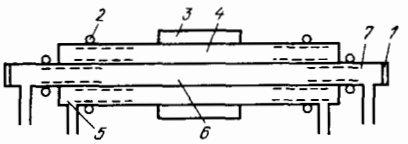

FIG. 10. Concentric heat-pipe oven for producing mixtures of two different metallic vapors:[85] 1—windows; 2—cooling chamber; 3—heater; 4—metallic vapor; 5—buffer gas; 6—active region: mixed metallic vapors; 7—buffer gas.

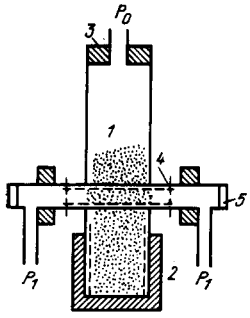

FIG. 11. Concentric heat-pipe oven with improved metallic vapor distribution along the oven.[87] 1—metallic vapor; 2—heater; 3—water cooling chamber; 4—diaphragm; 5—windows.

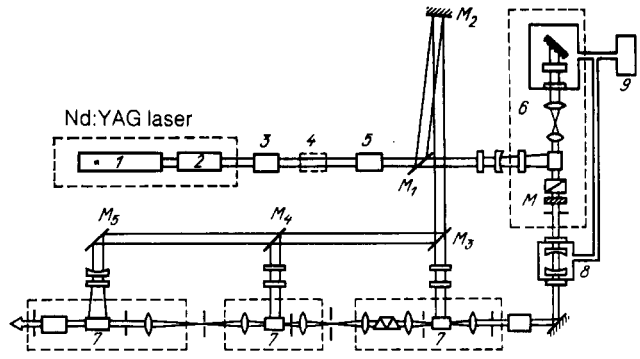

FIG. 13. YAG and dye laser system to generate intense, tunable UV radiation:[12] 1—YAG laser; 2—amplifier; 3—frequency doubler; 4—frequency tripler; 5—prism resonator; 6—dye laser; 7—dye amplifier; 8—confocal resonator; 9—vacuum chamber.

Losses of generated radiation to absorption outside the nonlinear conversion region are most important in the VUV range. In a two-photon resonance stimulated by a monochromatic pump the generated power is inversely proportional to the square of the resonance width. A collision-free gas of particles moving at the same speed can have a resonance width two to three orders of magnitude narrower than the Doppler-broadened width. This encouraged the technological development of pulsed, supersonic gas jets directed orthogonally to the laser beam.[14,89] In this scheme the jet cross section is comparable to the focal length and jet pulses are synchronized with laser pulses. Between two successive pulses the pumps have time to evacuate the gas from the vacuum region. The pulsed delivery conserves gas which is important when high-cost gases are employed. Supersonic gas jet technology permits atomic densities of the order of 10^{17} cm^{-3} in the jet and, simultaneously, maintains a vacuum of the order of 10^{-5} Torr in the chamber.[14] The nozzle ejecting the gas jets can be a millimeter or smaller in diameter; the jet cross section is of the same order. If molecular gases are used, their expansion cooling populates certain rotational levels in the jet to densities that are comparable to the total molecular density. This opens up new possibilities for molecular gas applications in nonlinear optics.

Photon energies in the VUV and SX are sufficient to dissociate most molecules and ionize atoms. Consequently such radiation is effectively absorbed by various media. The generation of such radiation requires careful selection of the nonlinear medium with low absorption and of appropriate oven windows. In the 100–200 nm range the best material for windows is LiF, which has a short-wavelength transmission threshold near 105 nm; the most widely used nonlinear materials are alkali earth metallic vapors (Sr, Mg, Ba, Hg, Zn, Ca, Be), noble gases (Ar, Kr, Xe, He, Ne), and some molecular gases with higher-lying electron transitions[90] (like NO, N_2, CO, H_2, and others). The ions of some elements with higher-lying discrete levels have also attracted attention.[91,92]

In the $\lambda < 100$ nm region, where there are no transparent window materials available, solutions include ovens with no exit windows and various methods of differentially pumping the gas away from the pipe exit,[13] as well as the aforesaid supersonic gas jet ovens.

The possibilities of complex organic molecular vapors[93] and hollow gas-filled waveguides[94] have also attracted attention.

The most popular pump sources are dye lasers and their higher harmonics combined with the harmonics of excitation lasers (Fig. 13).

Tunable alexandrite lasers appear promising. Shorter wavelength lasers are expedient for generating radiation with $\lambda < 100$ nm. Excimer lasers, which efficiently generate powerful UV and VUV radiation, are useful in that regard. Excimer laser beams cannot be used directly for pumping because of their spatial inhomogeneity and high divergence, but there exist several methods of improving and controlling

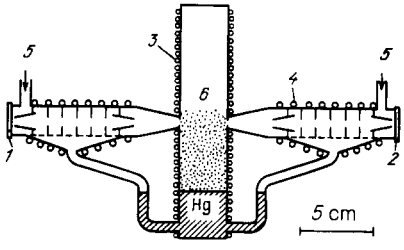

FIG. 12. Heat-pipe oven to produce mercury vapor:[88] 1—quartz window; 2—LiF-window; 3—heater; 4—cooling chamber; 5—gas intake; 6—Hg vapor.

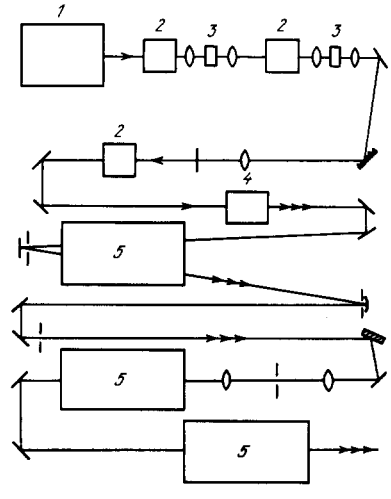

FIG. 14. Laser system based on THG in Sr vapor and an ArF* excimer amplifier to generate intense narrowband VUV radiation ($\lambda = 193$ nm) with low beam divergence:[216] 1—dye laser ($\tau_{pulse} = 10$ ps); 2—amplifier (dye); 3—saturable absorber; 4—Sr heat pipe; 5—ArF* amplifier.

excimer laser beam quality (see, for example, Ref. 95). One of the most promising methods involves the injection of radiation with specified parameters into the active medium of an excimer laser where it will be amplified. Excimer active media have high gain and sufficient spectral widths to amplify not only nanosecond, but picosecond and subpicosecond pulses to gigawatt levels. There have been major advances in this field.[13,24,113,214,215] In Fig. 14 we illustrate a laser set-up to generate powerful ($P = 4$ GW) picosecond pulses ($\tau_{\text{pulse}} = 10$ ps) at $\lambda = 193$ nm.[216] The output of a synchronously pumped, mode-locked dye laser ($\lambda \sim 580$ nm) is frequency tripled in strontium vapor to $\lambda = 193$ nm. The authors of Ref. 215 generated shorter pulses still ($\tau_{\text{pulse}} = 350$ fs) at $\lambda = 308$ nm.

4. GENERATION AND APPLICATIONS OF NARROWBAND TUNABLE VUV RADIATION

4.1. Characteristics of nonlinear optical converters

There are two experimental approaches to radiation conversion in GNM: 1) resonant and quasiresonant conver-

TABLE II. Generation of VUV and SX radiation by nonresonance frequency mixing in gases.

Wavelength, nm (generation spectral width)	Power generated or CF	Nonlinear/ synchronizing component	Nonlinear process	Pump lasers	References
206–160 ($\leqslant 3\times10^{-4}$ Å)	2–60W	Xe	$2\omega_{UV}-\omega_k$	YAG/dye (10 ns, ω_k: 4–5 MW; $\omega_{UV}=2\omega_k$: 1–1.7 MW)	148
195–163, 147–118	1 W (10^7 phot/pulse)	Xe	$2\omega_{UV}\pm\omega_s;\omega_i$	YAG ($\omega_{UV}=4\omega$; 30 ps, 20 MW) + PGS (ω_s,ω_i: 1 MW)	149
147–140	30 W (8.7×10^{10} phot/pulse)	Xe/Kr	$3\omega_k$	YAG/dye (10 ns, up to 2.6 MW)	150
130–110 (3×10^{-4} Å)	1–20 W	Kr, Xe	$2\omega_{UV}+\omega_k$	YAG/dye (10 ns, ω_k: 3–5 MW, $\omega_{UV}=2\omega_k$: 1–1.7 MW)	148
123.6–120.3 (4×10^{-3} Å)	up to 5 W	Kr	$3\omega_k$	N_2/dye (5 ns, 1 MW)	151
123.5–120.3	up to 16 W	Xe/Kr	$3\omega_{UV}$	YAG/dye (10 ns, ω_k: up to 5 MW; $\omega_{UV}=2\omega_k$: 1.5 MW)	150
121.6 (7×10^{-7} Å)	2.2 W (5.4×10^9 phot/pulse)	Kr	$3\omega_{UV}$	YAG/dye (5 ns, $\omega_{UV}=2\omega_k$:1.8 MW)	152
121.6	$\eta = 1.4\times10^{-4}$	Kr/Ar	$3\omega_{UV}$	Ruby/dye (10 ns, $\omega_{UV}=2\omega_k$:39 mJ)	153
121.6 (0.47 Å)	60 W (3.6×10^{11} phot/pulse)	Kr	$3\omega_{UV}$	YAG/dye (15 ns, $\omega_{UV}=2\omega_k$:10 MW)	154
121.6	$\eta\sim5\times10^{-5}$	Kr, Ar, Xe	$3\omega_{UV}$	$\omega_{UV}=2\omega_k$:10 MW)	155
121.6	35 W	Kr, Ar	$3\omega_{UV}$	Ruby/dye (20 ns, 2–5 MW)	156
121.6	100 W	Kr	$3\omega_{UV}$	XeCl*/dye (10 ns, 2 MW)	23a
118.2	$\eta\sim3\times10^{-3}$	Xe/Ar	$3\omega_{UV}$	YAG ($\omega_{UV}=3\omega$:35 ps, 400 MW)	157
118.2	260 W (4.7×10^{11} phot/pulse)	Kr, Xe (jet)	$3\omega_{UV}$	YAG ($\omega_{UV}=3\omega$:3 ns, 18 MW)	89
112.4 (0.3 Å)	0.8 W	Kr (4–5 atm)	3ω	N_2 (3 ns, 1 MW)	158
106.8–106.1 (~0.3 Å)	0.8 W	Xe	$3\omega_k$	KrF*/dye (2 ns, 2.4 mJ)	159
102.85–102.57	(1–10) mW	Ar	3ω	XeCl* (30 ns, 0.5 MW)	160
102.7	$\eta\sim10^{-9}$	Ar	3ω	XeCl* (10 ns, 12 mJ)	161
104.8–93.4 87–86.8 86.7–85.7	(1–8) W	Ar	$3\omega_{UV}$	YAG/dye ($\omega_{UV}=2\omega_k$:10 ns, 1–2 MW)	162
102.3–97.3 (1.9 cm^{-1})	7×10^9 phot/pulse	Ar jet	$3\omega_k$	YAG/dye 4 ns, 3–14 mJ)	163
88.7		Ar	$3\omega_{UV}$	YAG ($\omega_{UV}=4\omega$, 30 ps)	164
82.8		He, Xe (jet)	3ω	KrF* (15 ps, 20 mJ)	14
79 (~1 cm^{-1})	200 mW	H_2	$2\omega+\omega_k$	ArF* (10 ns, 10 mJ + dye (ω_k:10 ns, 5 mJ)	105
73.58–72.05	0.1–0.4 W	Ne	$3\omega_{UV}$	YAG/dye ($\omega_{UV}=2\omega_k+\omega_k$:0.3 MW)	165,12
64	20 kW	H_2	3ω	ArF* (10 ps, 10 mJ)	24
64	up to 30 W	H_2Ne, Ar, D_2, CO	3ω	ArF* (7 ps, 300 mJ)	166
64	$2\text{–}20\times10^4$ W	He, Ne, H_2, Ar, N_2, CO	3ω	ArF* (10 ps, 4 GW)	113

TABLE III. Generation of VUV and SX radiation by resonance frequency mixing in gases and metallic vapors (two-photon resonance, three-photon resonance, autoionization resonance: 2PR, 3PR, AR).

Wavelength, nm (generation spectral width)	Power generated or CF	Nonlinear/ synchronizing component	Nonlinear process	Pump lasers	References
220–155	0.5–1 kW	Xe	$2\omega_{UV} - \omega_k$	YAG/dye (10 ns, $\omega_{UV} = 2\omega_k$:0.3 MW, ω_k: 1.3 MW)	167
220–152	0.2–0.5 kW	Xe	$2\omega_1 - \omega_2$	YAG/dye (10 ns, ω_1: 80 kW, ω_2:100 kW)	168
200	100 kW	Ca	$3\omega_k$	dye (3 ps, 250 MW)	169
200	$\eta \sim 10^{-6}$	Na	$3\omega_k$	dye (2–4 ps, 2–3 GW)	170
200–190	$\eta \sim 10^{-5}$	Sr/Xe	$2\omega_1 + \omega_2$	Nd:glass dye (50 ps, 500 kW)	171
196–109	0.5–3 kW	Hg	$2\omega_1 + \omega_2$	YAG/dye (10 ns, 1–2 MW)	12,88
196–178	4×10^9 phot/pulse	Sr	$2\omega_1 + \omega_2$	N_2/dye (3 ns, ω_1: 15 kW, ω_2: 100 kW)	172
192	10^{10} phot/s	Sr	$3\omega_k$	Ar^+ + continuous dye	12
181			$2\omega_k + \omega_{Ar}$	(0.7–0.8 W)	
191	$\eta \sim 2\times10^{-5}$	Sr	$3\omega_k$	dye (500 ns, 40 kW)	173
185–125 (discrete)	up to 0.2 kW	Hg	$2\omega_{UV} = \omega_{VUV} + \omega_{IR}$ (decay)	YAG/dye (4 ns 20 mJ or (7 ns, 100 mJ)	174
173	0.2 kW	Mg/Xe	$\omega_{UV} + \omega + \omega$	Ruby (ω) ($\omega_{UV} = 2\omega$, ω: 50 MW, 10 ps)	175
170 (6 GHz)	10^7 phot/s	Sr	$\omega_1 + \omega_2 + \omega_3$	Ar^+ + continuous dye (ω_1:0.85 W; ω_2:0.42 W; ω_3:0.66 W)	176
176.5	4×10^8 phot/pulse	Ca	$2\omega_1 + \omega_2$	N_2/dye (3 ns, ~30 kW)	177
172–167	1.5×10^{-4} W ($\lambda = 169.7$ nm)	Sr	$2\omega_1 + \omega_2$	YAG/dye (5 ns, ω_1:320 W; ω_2:114 W);	178
	3.2 W ($\lambda = 171.2$ nm)		$\omega_1 + \omega_2 + \omega_3$	YAG/dye, ω_1:39 kW; ω_2:800 W; ω_3:3.6 kW)	
167	10^{12} phot/pulse	Ba^+ (inverted)	$2\omega_{UV} + \omega_1$	YAG/dye (10 mJ, 5 ns, ω_{UV}:1 μJ)	91
160–140 (0.1 cm^{-1})	60 W	Mg	$2\omega_1 + \omega_2$	N_2/dye (3ns, 30 kW)	179
155	100 W	Xe	$2\omega - \omega_k$	KrF* (10 ns, 25 kW) + XeCl*/dye (10 ns, 30 kW)	180
159	10 mW	Cd	$2\omega_{UV} + \omega_{IR}$	XeCl*/dye (ω_{UV}: ~6 ns, 4 mJ; ω_{IR}; 100 W)	181
152–130	10^7 phot/pulse	NO	$3\omega_k$	N_2/dye (3 mJ, 20 kW)	182
153.6	1 kW	Hg	$2\omega_{UV} - \omega$	Nd:glass ($\omega_{UV} = 4\omega$:0.4 ns; 0.1–1 MW; ω:10–100 MW)	65
143.6	$\eta \sim 10^{-4}$	Mg/Kr	$3\omega_k$	N_2/dye (3 ns, 30 kW)	183
143 (0.44 cm^{-1})	1.2×10^5 phot/s	Mg/Kr	$3\omega_k$	Ar^+/continuous dye (0.2 W)	12
140–146 (0.3 cm^{-1})	10 W	Xe	$\omega_1 + 2\omega_2$	YAG/dye (ω_1:8 ns, 3–5 mJ; ω_2:30 mJ)	185
140–106	up to 10^7 phot/pulse	Zn	$2\omega_1 + \omega_2$	KrF*/dye (12 ns, 10 kW)	186
129–121	10^8 phot/pulse ($\lambda = 121.6$ nm)	Mg	$2\omega_1 + \omega_2$	KrF*/dye (10 ns, 10 kW)	187
135.3–128.7	8×10^6 phot/pulse	Cd/Ar	$2\omega_{UV} + \omega_k$	YAG/dye ($\omega_{UV} = 2\omega_k$, $\omega_{UV}\times10$ kW, 5 ns, ω_k: 10 kW, 4 ns	188
127 (0.6 cm^{-1})	$\eta = 10^{-3}$–10^{-4}	Mg	$2\omega_k + \omega$	dye (7 ns, 1 mJ + XeCl* (15 ns, 6 mJ);	189
115 (0.3 cm^{-1})		Mg/Xe		dye + KrF* (15 ns, 80 mJ)	
125–122 (0.04 cm^{-1})	10 kW	Hg	$2\omega_1 + \omega_2$	YAG/dye (10 ns, ω_1: 30 mJ, ω_2:1–5 mJ)	190
125.9–74.8 (discrete)	(71.5–3) W	Xe	$3\omega_1$ $2\omega_1 \pm \omega_2$	YAG/dye	191
123.6	$\eta \sim 10^{-6}$	Mg^+	$2\omega_{UV} + \omega$	YAG/dye ($\omega_{UV} = 2\omega_k$: 10 ns, 0.05 mJ) + YAG (15 ns, 2.5 mJ)	92
123–121	$\eta = 3\times10^{-7}$	Be	$2\omega_{UV} + \omega_k$	YAG/dye (5 ns, $\omega_{UV} = 2\omega_k$:0.5 mJ; ω_k:0.1 mJ)	192
122–117	2×10^9–2×10^{11} phot/pulse	Hg	$2\omega_1 + \omega_2$	YAG/dye (10 ns, ω_1:0.8 mJ, ω_2:0.2 mJ)	193
120.3 (16 Å)	300 W	Hg	$2\omega_k + \omega_{UV}$	dye (6 GW/cm^2) + 4ω YAG (650 MW/cm^2)	194
117	~1 mJ	Xe	3ω	XeF* (20 ns, 7×10^{12} W/cm^2)	195
115	up to 20 W	CO/Xe	$2\omega_{UV} + \omega_k$	YAG/dye ($\omega_{UV} = 2\omega_k$: 8 ns, 5 mJ; ω_k: 30 mJ)	196
97.2	$\eta \sim 10^{-9}$	H_2	$3\omega_{UV}$	N_2/dye ($\omega_{UV} = 2\omega_k$: 5 ns, 50 kW)	197

TABLE III. (*Continued.*)

Wavelength, nm (generation spectral width)	Power generated or CF	Nonlinear/ synchronizing component	Nonlinear process	Pump lasers	References
96.7–93.5	5×10^9 phot/pulse	N_2, CO	$3\omega_{UV}$	YAG/dye ($\omega_{UV}=2\omega_k$, ω_k:2–3 mJ, 10 ns)	90
93	up to 0.05 μJ	Hg	$3\omega_k$	dye (5 ns, up to 20 mJ)	198
83			$2\omega_1+\omega_2$		
89.6	$\eta\sim10^{-6}-10^{-9}$	Hg	3_{UV}	Nd:glass ($\omega_{UV}=4\omega$: 50 ns, 1 MW)	199
82.8–83.3 (0.01 cm^{-1})	up to 40 mW	Xe	3ω	KrF* (10 ns, 60 mJ)	200
57 (0.8 Å)		Ar	3ω	Xe_2 (10 ns, 1 MW)	201

sion, using low pumping field intensities and low atomic concentrations (to suppress limiting factors); 2) nonresonant conversion, wherein high pumping intensities and higher atomic concentrations are required. The concrete problem at hand and the concrete experimental conditions determine the proper approach.

The results of experimental research and development of methods of generating coherent, tunable VUV radiation in GNM can be summarized as follows (see, for example, Refs. 11, 96 and references therein).

In the case of nonresonance conversion, in a field of approximately 10 ns pulses of several megawatts, the CF of cubic nonlinearities is usually of the order of 10^{-4}–10^{-5}, and the generated power is measured in tens or hundreds of watts. In a field of 10 ps pulses of about 1 GW the CF reaches 10^{-3}–10^{-5} and the generated power reaches tens or hundreds of kilowatts.

Using the two-photon resonance in a field of nanosecond magawatt pulses the CF of cubic nonlinearities grows to a fraction of a percent and 1–10 kW of power are generated. In the c.w. regime VUV beams of about 10^{10} photons/s with a bandwidth of less than one MHz have been achieved. In quasiresonance conversion using $\chi^{(5)}$ with picosecond gigawatt pulses the CF may become of the order of 10^{-5}–10^{-6} (see, for example, Ref. 97); on the $\chi^{(7)}$ nonlinearity CF may reach 10^{-7}–10^{-8}. In a number of cases—Hg is an example—the CF can be higher by one or two orders of magnitude.[16] In the resonance case the CF of even $\chi^{(9)}$ can reach 10^{-5}.[16] VUV power generated on higher nonlinearities lies in the range from hundreds of watts to several kilowatts.

Anti-Stokes scattering of ArF* laser radiation from the H_2 molecule yields lines up to the sixth order: $\lambda=179$ nm, 168 nm, 156 nm, 146 nm, 138 nm, and 130 nm of 270–0.8 kW power and several nanoseconds duration.[15] In recent years several laser set-ups have been based on anti-Stokes Raman scattering from excited atoms and molecules in metastable states, with $\lambda<200$ nm (see, for example, the review by Popov[95]).

At present, nonlinear optical methods of gaseous media have rendered the entire 200–100 nm range accessible, as well as parts of the 100–35 nm range, with generated powers sufficient for many applications. The achieved results in VUV and SX radiation using GNM are summarized in Tables II–IV (see also Figs. 15, 16).

4.2. Comparison of nonlinear optical and non-lasing sources of VUV radiation

Tunable coherent VUV radiation significantly broadens the opportunities of studying continuous absorption and photoionization spectra, as well as Rydberg and autoionization states. Vacuum ultraviolet radiation at the 200–100 nm

TABLE IV. Generation of UV, VUV, and SX radiation by frequency mixing on higher nonlinearities.

Wavelength, nm (generation spectral width)	Power generated or CF	Nonlinear/ synchronizing component	Nonlinear process	Pump lasers	References
215.4	2 kW	Cs	$\chi^{(5)}$, 5ω	Nd:glass (50 ps, 0.1 GW)	97
212	4 kW	Na/Xe	$\chi^{(5)}$, 5ω	Nd:glass (10 ps, 63 mJ)	202
153.7–151	0.1 kW (10^{13} phot/pulse)	Hg	$\chi^{(9)}$,$8\omega-\omega$, 8PR	Nd:glass (0.4 ps, 10–100 MW)	16
151	$\eta\sim10^{-11}$	Na	$\chi^{(7)}$, 7ω	Nd:glass (10 ps, 63 mJ)	203
139.3–137.5	10 W	Xe	$\chi^{(5)}$ $\omega_1+3\omega_2-\omega_2$	YAG/dye (8 ns, 3–30 mJ)	185
117.7	$\eta\sim10^{-16}$	Na/Ar	$\chi^{(9)}$, 9ω	Nd:glass (10 ps, 63 mJ)	203,204
76; 71; 62.6; 59.1		He, Ne	$\chi^{(5)}$ $4\omega_{UV}\pm\omega_2$	YAG ($\omega_{UV}=4\omega$; $\omega_2=\omega$, 2ω)	205
61.6	$\eta\sim10^{-10}$	Ar, Kr	$\chi^{(5)}$, 5ω	XeCl* (3–10 ns, up to 40 MW)	206
53.2	$\eta\sim10^{-5}$–10^{-6}	Ne, He	$\chi^{(5)}$, $5\omega_{UV}$	YAG ($\omega_{UV}=4\omega$:30 ps, 330 MW)	205
49.7		He, Ne	$\chi^{(5)}$, 5ω	KrF* (15 ps, up to 20 mJ)	14
38.6	up to 200 W	H_2, He, Ar, N_2, CO	$\chi^{(7)}$, 5ω	ArF* (10 ps, 4 GW)	113
38	$\eta=10^{-7}$–10^{-8}	He	$\chi^{(7)}$, $7\omega_{UV}$	YAG ($\omega_{UV}=4\omega$:30 ps; 330 MW)	207
35.5	$\eta\sim3\times10^{-11}$	He	$\chi^{(7)}$, 7ω	KrF* (15 ps, up to 20 mJ)	14

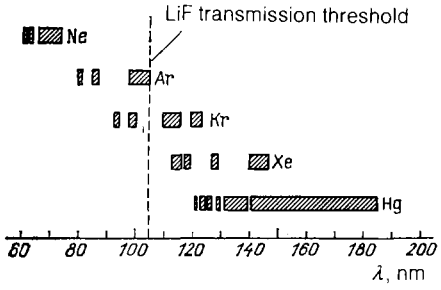

FIG. 15. Regions of third harmonic wavelengths where the dispersion $\Delta k = k_3 - 3k_1$ is negative in Ne, Ar, Xe, and Hg.[12]

range is proving most useful for these purposes. Since methods of obtaining tunable, narrowband VUV radiations accessible to many physics laboratories have been developed only quite recently, there has been much less high and ultrahigh resolution linear and nonlinear spectroscopic research in this spectral range than in the visible and near UV ranges.

Traditional VUV spectroscopic techniques employ gas discharge lamps (noble gases or hydrogen) and vacuum monochromators. More intense synchrotron sources that yield high resolution also require vacuum monochromators. The resolution attained by such technology is determined by the particular machine used. The record resolving power $R = \lambda/\Delta\lambda$ was achieved using a 10.7 meter VUV spectrograph with a diffraction grating[98] (0.4 Å/mm dispersion, $\Delta\lambda = 0.2$–$0.3\ \text{cm}^{-1}$ at $\lambda = 100$ nm, $R = (3$–$5)\cdot 10^5$).

A single-mode laser has a much narrower spectral range than the best diffraction grating or Fabry-Perot interferometer. Hence the attraction of VUV laser sources, which possess a number of unique qualities: high intensity, very narrow spectral linewidth, temporal and spatial coherence, and, if necessary, short pulse duration. Only a few types of lasers provide radiation at several discrete frequencies in the $\lambda < 200$ nm range. Progress in the generation of tunable radiation in a wide range below 200 nm is entirely due to utilization of nonlinear optical phenomena in gases. The typical resolving power of such sources has already reached $(1$–$5)\cdot 10^5$ and the record stands at 10^7.[19] The generated radiation is not only sufficiently intense for linear spectroscopy, but also for multiphoton excitation of atoms and molecules. In the past few years much progress and a number of important results in spectroscopy and photophysics have been achieved by using GNM-based VUV sources. The new research opportunities are regularly discussed at international conferences devoted to applications of VUV and SX radiation.

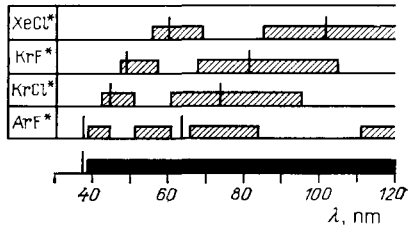

FIG. 16. VUV and SX radiation wavelengths obtained by $\chi^{(3)}$ and $\chi^{(5)}$ frequency mixing using excimer lasers (λ) and dye lasers (λ_d) (217 nm$\leqslant\lambda_d\leqslant$750 nm):[13] $\lambda/3$ and $\lambda/5$ are marked.

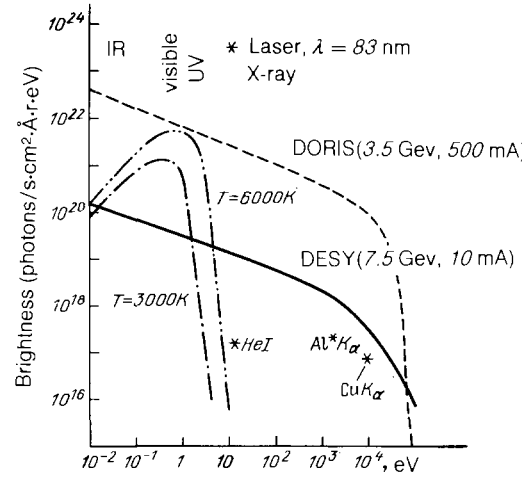

FIG. 17. Spectral brightness comparison between incoherent synchrotron and lamp sources and a laser source.[24] The dash-dotted line traces the black-body radiation brightness.

Before proceeding with concrete examples, let us briefly compare the spectral brightness of various VUV light sources. In Fig. 17 we plot the spectral brightness of several sources over various spectral ranges, the sources including a VUV lamp, the DORIS and DESY synchrotrons, and third harmonic radiation of a KrF* laser.[24] These results demonstrate that the spectral brightness of the third harmonic ($\lambda \approx 83$ nm) exceeds that of other sources by at least an order of magnitude. Spectral brightness of $3\cdot 10^{31}$ phot/s·cm²·Å·sr has been attained at $\lambda = 143.6$ nm. Sum frequency generation can achieve the same order of spectral brightness over the entire 100–200 nm frequency range. At the $\lambda = 53$ nm wavelength the brightness reaches $6\cdot 10^{30}$ phot/s·cm²·Å·sr.[10] The total number of photons radiated by arc lamps is of the same order as by lasers, but the spectral brightness of a lamp is much smaller because of great beam divergence and radiation spectral width.

4.3. Applications of nonlinear optical sources of VUV radiation

Vacuum ultraviolet radiation is important to the studies of molecular spectra. The first linear spectroscopic ex-

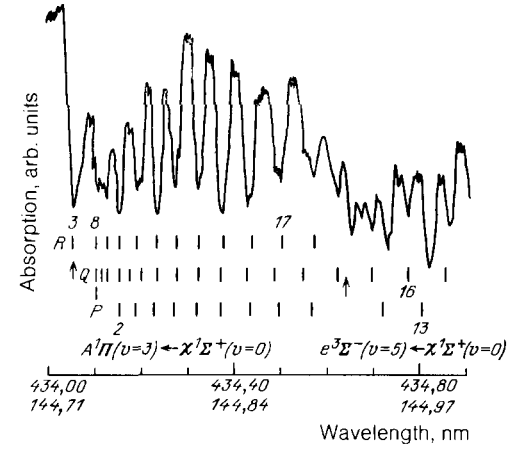

FIG. 18. Absorption spectrum of CO near $\lambda = 144$ nm using the third harmonic generated in Xe.[22] Upper scale—laser wavelength in air; lower scale—VUV wavelength corrected for air refraction.

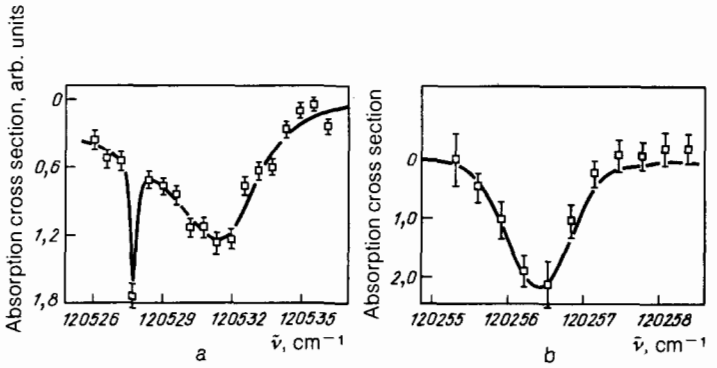

FIG. 19. Examples of high resolution absorption spectra in D_2 (a) and H_2 (b) near $\lambda = 83$ nm (third harmonic of KrF laser in Xe).[20] a—Broad asymmetric transition $D \leftarrow X(5,0)R(2)$ in D_2. Solid line is the convolution of Doppler and Fano profiles. b—Narrow symmetric transition $D'' \leftarrow X(0,0)R(1)$ in H_2. Solid line is the Gaussian profile with Doppler width.

periments followed the successful generation of VUV radiation by frequency mixing in Sr and Mg vapors. The absorption spectrum of the O_2 molecule was reported in Ref. 99, that of the CO molecule in Ref. 22 (Fig. 18, also Refs. 100, 101). Detailed investigations of the VUV spectra of NO and CO were carried out by Vidal.[102] In many cases relatively simple experimental set-ups yielded rotational spectra of fairly high resolution. The Lyman absorption spectra of H and D atoms were obtained in Ref. 103. The authors of Ref. 20 obtained high resolution spectra ($\Delta\tilde{\nu} \approx 0.2$ cm^{-1}, $R = 6 \cdot 10^5$) of H_2, D_2, and HD molecules in the 83 nm region (Fig. 19). On the one hand, these molecules, particularly H_2, are the simplest, on the other hand their study is of fundamental importance to the development of theoretical physics and chemistry, and the many practical applications. These experiments were probably the first to demonstrate the possibilities of high resolution spectroscopy in the far VUV range. The absorption spectrum of H_2 in the 97.3–102.3 nm range was reported in Ref. 104. Spectroscopic research at even shorter wavelengths was carried out by Srinivasan and co-workers,[105] who recorded Al resonance spectra near 79 nm in D_2 and Ar (Fig. 20). Absorption spectra of K near 54 nm with 1.9 cm^{-1} resolution ($R \approx 10^5$) were reported in Ref. 21.

One of the applications of tunable VUV radiation near the Lyman α and β lines is the probing of hydrogen plasma used for thermonuclear fusion. Power of the order of 10–100 kW and bandwidth of less than 1 Å are required to measure plasma densities in the 10^7–10^8 cm^{-3} range.[107] The first experiment to measure atomic concentration and velocity distribution of H and D in a Tokamak hydrogen plasma was reported in Ref. 23a. Pulse power of 100 W at $\lambda = 121.6$ nm attained concentration sensitivity down to $N \approx 10^9$ cm^{-3}. The H and D Lyman lines in this experiment were broadened to ~ 1 cm^{-1}.

The potential applications of VUV radiation generated by nonlinear mixing in the field of chemical physics have been demonstrated by experiments measuring the radiation lifetimes of rotational levels in the $v = 0$ vibrational state of the first excited electron level in CO and directly measuring the H + Br scattering cross-section as a function of the kinetic energy of the H atom.[18]

A number of studies of photoionization spectroscopy using VUV radiation have been carried out by the authors of Ref. 18. In particular, they studied the single photon ionization of NO near 123 nm and selective two-photon ionization of CO (ionization potential of 14.0139 eV). In the latter case VUV radiation (the third harmonic of a laser with $\lambda = 368$ nm) was employed for preliminary excitation of the CO molecule into the $v' = 13A\,^1\Pi_1$ state with subsequent ionization using the fourth harmonic of a YAG laser. The resolution of this ionic spectrum was 0.55 cm^{-1}. Similar experiments were carried out on NO molecules.[22] The photoionization of H and D atoms was attained by analogous methods, using VUV radiation to excite the atoms into the 2^2P state. The hyperfine structure of the H ground state (1^2S) has also been studied. Other authors investigated the possibility of obtaining polarized protons by means of a two-photon ionization. Two-step excitation of Rydberg states in hydrogen atoms has been accomplished:[108] $H(1^1S) + \hbar\omega_{VUV} \rightarrow H(2^2P) + \hbar\omega_{UV} \rightarrow H(n^2S,\ n^2D) \rightarrow H^+_{ion} + e^-$. The resonance two-photon ionization of H_2 has been studied using VUV radiation at $\lambda = 111$ nm, with $B\,^1\Sigma^+$ ($v = 0$) as the resonance intermediate state. The dynamics of IR multiphoton excitation, subsequent photoionization and dissociation of the $(CH_3CO)_2O$ has been investigated

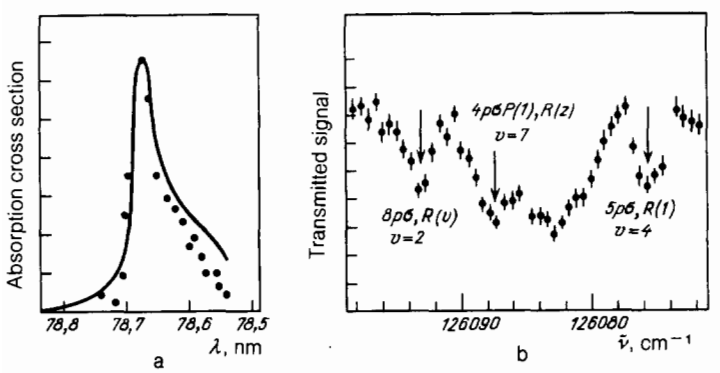

FIG. 20. Absorption spectra of transitions to autoionization states near $\lambda = 79$ nm.[105] The VUV radiation was generated by mixing ArF laser radiation with tunable dye laser radiation ($\lambda_d = 436$ nm), $\omega_{VUV} = 2\omega_{ArF^*} + \omega_d$, a—Ar absorption in the transition to $2P_{1/2}9d$, b—D_2.

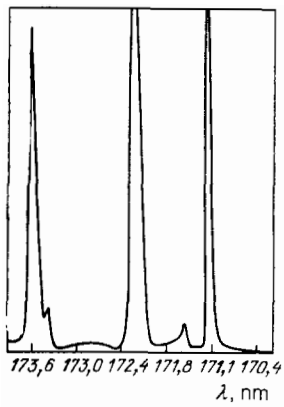

FIG. 21. Typical spectral dependence of VUV radiation intensity generated by four-wave mixing in Sr vapor.[46]

using VUV radiation with $\lambda \approx 118.4$ nm. The same method can be used to study the dissociation kinetics and dynamics of excited electronic states in complex molecules—information currently unavailable for most molecules.

Two-photon VUV excitation of Ar atoms in the $\lambda < 100$ nm range was investigated by Wallenstein.[12] That experiment demonstrated the utility of VUV radiation obtained in GNM media for nonlinear excitation of atoms and molecules. Since resonance conversion can generate sufficiently intense VUV radiation in the 200–100 nm spectral range, nonlinear optical excitation can be utilized for spectroscopic research in the 100–50 nm range. Today there is every reason to transfer the expertise of nonlinear laser spectroscopy from the IR and visible to the VUV and SX ranges.

The potentialities of generation VUV spectroscopy in molecules using third-order susceptibility was demonstrated in Ref. 109; higher-order susceptibilities were employed in Ref. 110. This method can also be applied to spectroscopy of Al resonances in atoms[46,47,111] (Fig. 21) and predissociation states in molecules to gather information that cannot be obtained in any other way. In particular, one gains the possibility of studying the detailed structure of nonfluorescent electron rotational states.[109]

In addition to spectroscopy, VUV radiation holds promise in the areas of holography[25] and microlithography.[112] The development of coherent VUV sources with $\lambda < 100$ nm and high spectral brightness, based on KrF* and ArF* amplifying systems that can work on picosecond time scales, opens up additional possibilities in research and applications that require precisely such sources. Some of these applications are discussed in Refs. 24 and 113. The authors of Ref. 24 propose to use $\lambda = 83$ nm radiation in laser processing of semiconductors for microelectronic components. There has been discussion of studying surface phenomena in condensed matter with high temporal and spatial resolution, for example to probe the recrystallization process after laser annealing in semiconductors. It is predicted that 10 ps pulses of up to 100 kW will detect individual atomic layer formation. Other important applications include the diagnostics of intertial thermonuclear plasma.[113] Various estimates indicate that narrowband, spatially coherent VUV radiation with $\lambda < 100$ nm will significantly reduce power requirements for pulsed photography of such objects in comparison with x-ray radiation.

The above list in no way exhausts the possible applications of tunable coherent VUV and SX radiation. Nonetheless, even the cited reports demonstrate the practical importance of developing and improving VUV and SX generation technology in gaseous media.

5. CONVERSION OF EXCIMER LASER FREQUENCIES TO THE BLUE-GREEN SPECTRAL RANGE

Generation of powerful radiation in the blue-green region of the spectrum $\lambda = 450$–530 nm using SRS of excimer lasers in alkali earth vapors and molecular gases has attracted much interest in recent years.[114] This interest is due to several important applications. For example, in this range sea water is relatively transparent; many biological objects have absorption bands; dye lasers can be effectively pumped; a number of other applications exist. The quantum efficiency of SRS of excimer laser radiation in metallic vapors can reach 80%[115] and the energy output of the Stokes component approaches 1 J.[116] The small Stokes shifts in molecular gases make it necessary to use higher order scattering. Adequately efficient conversion has been observed up to the sixth order.[117] An amplifier-equipped system reached conversion efficiency of up to 47% into the second Stokes component ($\lambda = 500$ nm).[118] Stimulated Raman scattering in GNM may also hold some promise for pulse compression.[119]

6. SOURCES OF TUNABLE NARROWBAND IR RADIATION

6.1. SERS in metallic vapors

The most widely used method of generating IR is by SERS; the most convenient atomic medium for SERS is alkali metal vapor. Research has shown that for efficient conversion the pump wavelength should lie in the vicinity of some allowed single photon resonance and that of all the KP transitions S–S transitions work the best. In that case the gain coefficient is maximized if the intermediate state is chosen to be a P state with the same principal quantum number as the excited level. In some experiments several tens of kilowatts of pumping power resulted in IR radiation tunable over several hundred cm^{-1} with peak quantum efficiency up to 50%. For example, in SERS on the 6S–7S transition of the Cs atom[120] the pump was tuned near the $6S$–$7S_{1/2,3/2}$ transition (Fig. 22): that experiment registered tunable IR radiation in the 2.67–3.47 μm frequency range with peak power of up to 1 kW.

The generated radiation was used to study the absorption spectra in CH_4 and ammonia with resolution no worse than 0.4 cm^{-1}. More powerful pump sources[121] resulted in a

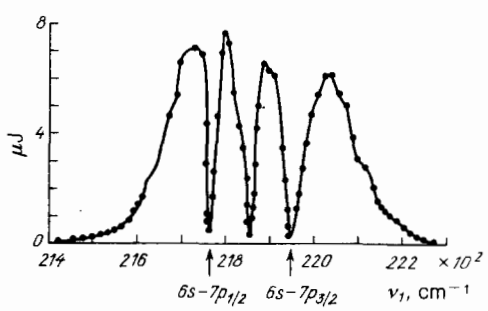

FIG. 22. Dependence of IR pulse energy on pump frequency in SERS in Cs vapor using the 6s–7s transition.[120]

tunable region of 2.5–4.7 μm with peak power up to 25 kW; whereas 6S–8S and 6S–9S transitions yielded IR radiation in 5.67–8.65 μm and 11.7–15 μm ranges with power up to 7 and 2 kW respectively. As long as the Doppler broadening of the transition was much smaller than the pump spectral width, a typical laser pump spectral width $\Delta\nu_1 < 0.1$ cm^{-1} translated into an SERS line 0.3–1 cm^{-1} wide.

The development of powerful UV lasers, particularly of the excimer variety, made possible IR generation by SERS in the 20 μm and higher wavelength range, including SERS on transitions to Rydberg states. This opened up possibilities of generating tunable far infrared radiation. However, the conversion efficieny of such processes is small because of the small factor ω_{IR}/ω_1. An alternative method of generating far IR radiation involves SERS between excited states (Rydberg states, for example). It is most advantageous to use transitions from the first excited P state, which can be populated in different ways. The effective lifetime of these states in alkali metal vapors is sufficiently high (of the order or microseconds) for radiation trapping. This method was applied to K vapor to generate IR radiation in the 8.5 and 16 μm regions using the 4P state populated by supplemental laser radiation.[122] In another experiment the 4P state in K vapor was populated by glow-discharge.[123] The authors observed that the number of photons generated per pulse in the 16 μm region exceeded the population of the 4P state by more than an order of magnitude. This occurs because the same atom interacts with the radiation several times during each pulse (because of the quick decay to the 4P state), significantly enhancing the CF in the process.

The possibility of generating intense IR picosecond pulses via SERS deserved further study. This technique was first attempted in Ref. 124 using SERS in Cs vapors. Wyatt and Cotter[125] generated picosecond IR radiation ($\tau = 30$ ps, $\lambda = 2.38$ μm) with quantum CF $\sim$20%. In addition to SERS, resonant four wave mixing processes in gaseous media are also used to generate tunable IR radiation. The most common four wave mixing methods employ the Raman resonance $\omega_{IR} = |\omega_4 - \omega_2 - \omega_3| = |\omega_{ng} - \omega_1|$ (Fig. 1d). When an electron transition is employed as the n–g atomic transition the generated power is usually low, but the generated radiation is tunable in a wide range from a few microns to tens of microns. Pump power in the kilowatt range generates a fraction of a watt at a few microns to a fraction of a milliwatt at tens of microns.[126]

6.2. SRS in molecular gases

Compared to SERS in atoms SRS in molecular gases is a process characterized by less resonance. This permits a wider tuning range in the infrared. The long wavelength generation threshold ($\lambda > 2\,\mu$m) can be significantly lowered by means of multiple-pass or waveguiding cells (Ref. 127 and references therein). By working with molecular gases (H_2, N_2, and others) it is possible to generate radiation in the near (1–10 μm), middle (10–18 μm), and far (40–250 μm) infrared.[128] In particular, generated power of 1–200 MW was reached in the near IR and 1.7 mJ per pulse at 16 μm. When using vibrational molecular transitions it is convenient to use a biharmonic pump $\omega_{IR} = \omega_1 - \omega_{ng} = \omega_1 - (\omega_4 - \omega_3)$ because the tunable radiation does not need to be intense and the generation threshold is lowered when the molecules are vibrationally excited by intense radiation at a fixed frequency ω_4. For example, Ref. 129 reports on the generation of tunable IR radiation in H_2 by using a parametric light generator (ω_1) and intense YAG laser radiation ($\lambda_4 = 1.06\,\mu$m). The tunable radiation was subsequently applied to study the absorption of polystyrene in the 769–2400 cm^{-1} range.

6.3. THG on vibrational molecular nonlinearities

One method of generating intense tunable radiation in the 2.7–3.5 μm range (the region where the frequencies of C–H, O–H, and N–H bonds are concentrated) is third harmonic generation of high-output tunable CO_2 and CO laser radiation on vibrational nonlinearities of such molecules as H_2, HCl, SF_6, DCl, CD_4, C_2H_4, NH_3, OCS and others. Although theoretical estimates predict peak CF of about 10%[130] the highest CF attained to date is 4% in cryogenic CO–O_2 liquid solution with SF_6 added for phase matching.[131] In gaseous molecular media the best results were reported in Refs. 132 and 217, with the record (in terms of energy) CF $\sim$0.1% obtained by converting CO_2 laser radiation into the 3 μm region on vibrational nonlinearities of molecular ozone. The liquid phase has the advantage of high active particle concentration and uniquely narrow two-photon absorption lines due to the motional-narrowing effect.[133] A concise review of nonlinear optics in cryogenic liquids is available in Ref. 134.

Resonant harmonic generation and frequency mixing on vibrational nonlinearities of molecular gases and liquids is useful in nonlinear spectroscopy, yielding information that is inaccessible by ordinary linear spectroscopic means.[135]

7. UPCONVERSION AND ADVANCES IN IR RADIATION DETECTION

The frequency upconversion of weak IR signals into the visible and near UV regions of the spectrum has attracted interest for many reasons. In the visible range effective, low-noise photodetectors with high temporal resolution are readily available, whereas the sensitivity of IR detectors is lower by 7–8 orders of magnitude and the temporal resolution is much poorer. Also, visible range detectors usually work at room temperature, whereas IR detectors require cooling to low temperatures. Consequently, detection and analysis of IR signals by way of their preliminary conversion into the visible and UV spectral ranges enjoys all the advantages: quick response, broad bandwidth, high sensitivity, and accurate wavelength measurement. The converted signal retains, for the most part, the information contained in the spatial, temporal, and spectral characteristics of the original IR radiation. Hence, upconversion of IR radiation into the visible range results in major advances in optical ranging and communication, IR spectroscopy and astronomy, metrology and IR holography. For example, even fairly ineffective conversion makes it possible to construct IR detectors working on pico- and femtosecond time scales to study rapid processes in biology and chemistry.

Upconversion methods employ physical processes in which an IR photon combines with one or two laser pump photons to create a photon in the visible or near UV range. We will only consider coherent (parametric) interaction of IR and laser pump radiation in metallic vapors which leads to sum frequency generation.

Until recently researchers have concentrated on para-

metric mixing processes in crystals with typical conversion efficiencies of 10^{-4}–10^{-6} for continuous wave radiation and several tens of percent for pulsed radiation (modulated Q factor regime) (see, for example, Ref. 136).

Gaseous nonlinear media have several advantages over crystals in the field of IR upconversion and permit solution of some problems which are poorly, if at all, adapted to crystals. First, with the exception of several narrow lines gaseous atomic media are transparent throughout the IR range. Second, as we have noted already, the pump and converted frequencies are sufficiently separated to make for easy filtering of the weak signal from the strong pump. Third, there is no limitation to the aperture of the nonlinear medium and the technology of vapor production is relatively simple and cheap. Fourth, the high radiation resistance of GNM make it possible to use powerful pump pulses of greater duration than in crystals.

Atoms of alkali metals are well adapted to convert signals to the visible and near UV spectral ranges because they have the lowest-lying excited states with sufficiently high oscillator transition strengths. There are several methods of raising the frequency of IR radiation by nonlinear resonance mixing in GNM. All these methods are variations of two major types: two-photon resonance at pump frequencies[3,4] (see Fig. 1a) (Raman scattering can also be used with SERS serving as the second pump) (see Fig. 1d) or two-photon resonance at the sum frequency of one of the pumps and the IR radiation—the so-called complementary scheme in which the IR frequency is boosted to resonance by the pump.

Various investigations have shown that effective conversion by two-photon pump schemes requires several conditions to be satisfied simultaneously, the more important of these conditions being the existence of a two-photon resonance at the pump frequency and a quasiresonance at the sum frequency. Phase matching should hold in the $N \sim 10^{16}$–10^{17} at·cm^{-3} range. These simultaneous conditions are easily satisfied if there are no restrictions on the desired frequency of the IR radiation. The IR frequencies that can be efficiently converted in a given GNM are then fixed and determined by the energy spectrum of the medium. Thus, by using the proximity of the P(40) ($\lambda = 10.8\,\mu$m) line in the widely used 10 micron generation band of the CO_2 laser to the $6S$–$6P_{3/2}$ transition of the Na atom (the detuning from resonance being $\Delta\nu = -0.14$ cm^{-1}), Makarov and coworkers[4] obtained a quantum CF of 65% with respect to IR radiation density passing through the pump beam cross-section (and a power CF of 2640%). The wavelength at the sum frequency was $\lambda = 268\,\mu$m at a pump power of several kilowatts.

The complementary scheme arrangement for the two-photon resonance removes the restrictions on converted IR frequencies and opens up great possibilities for IR signal imaging in a wide spectral range, including the frequencies of existing IR lasers. This advance is due to the fact that by tuning the second pump frequency near the three-photon resonance it is possible to vary the phase matching condition and reach optimal sum frequency generation. This method permits the conversion of any IR radiation via a single nonlinear medium and can serve as the foundation of an IR spectrometer. Theoretical analysis places a probable quantum CF limit of no higher than 25% on this scheme because of parametric brightening in the medium. But the power CF can exceed 100%. The first experiment based on this scheme[6] yielded a CF of 10^{-4}%. In Ref. 138 the quantum output already reached about 12%, even though the optimal conditions were not completely implemented. In that experiment weak $\lambda = 1.06\,\mu$m radiation was converted to the 322.9 μm region in Rb vapor pumped by two dye lasers of several kilowatt power.

Sum frequency generation in a continuous regime is also of great interest. Such an experiment was reported in Ref. 17: CO_2 laser radiation ($\lambda = 10.8\,\mu$m) was converted in Na vapor to 268 nm with a power CF of 9% with respect to IR radiation traversing the pump beam cross-section. The process used was two-photon excitation in the laser field of an Ar laser and a dye laser. In the case of relatively weak pump fields it was demonstrated that tuning the pump to an intermediate single-photon resonance yields the best results, despite the enhancement of competing processes.

Thus we find that for optimal conditions the required pump power is several orders of magnitude lower in GNM than in nonlinear crystals.

Nonlinear frequency mixing in GNM opens new vistas in the fields of IR imaging and thermal radiation detection. Only a few experiments in IR imaging have been carried out to date. For instance, in Ref. 6 the upconversion of $\lambda = 2.94$ μm radiation of 0.4 μm in Cs vapor permitted a resolution of $1.6 \cdot 10^4$ spots with an energy CF of 32%. The Cs vapor IR radiation converter described in Ref. 5 performs as well as the best crystal-based machines, but its pump power requirement is lower by two orders of magnitude ($\approx 10^5$ W/cm^2). This device can image an object 40 meters in diameter at a distance of 3 km.

Let us compare the various IR detection methods on the basis of available research results.[139] The active upconversion and imaging of IR radiation (when the objects are irradiated with IR lasers) has advantages over all other methods. Yet in the passive case (that is, when thermal images are converted) quantum counters and IR detectors have better characteristics than upconverters. This happens because most nonlinear detectors are currently pumped by pulsed lasers with relatively low repetition rates, resulting in the overall low conversion efficiency of continuous IR signals. In the active mode the detected radiation is also the pulsed radiation and is synchronized with the pump, which results in much better conversion efficiency. In the case of thermal imaging direct detection methods are preferable to all the rest. Quantum counters are very sensitive to thermal radiation but have much less resolving power than frequency converters. Metallic vapors perform better than crystals both in the active and in the passive conversion techniques. The efficiency of frequency mixing in the continuous regime can be enhanced by positioning the cell containing the nonlinear medium inside a running wave resonantor—this is especially important for thermal radiation conversion.

As we have noted already, the conversion of IR to higher frequency is finding more and more applications. The promising features of IR spectrum photography with temporal resolution, based on upconversion to the visible range, have been demonstrated in Ref. 7. The method is based on generating wideband IR radiation by SERS in metallic vapors, the subsequent absorption of this radiation by molecular media containing chemical reaction products, and finally the upconversion of this wide band (of the order of several

TABLE V. Conversion of IR radiation into the visible and UV spectral ranges in metallic vapors.

λ_{IR}, μm	λ_s, μm	Quantum CF η_q, power CF η_p	Nonlinear medium	Process, order of resonance	Lasers	References
9–11	0.3	max $\eta_q = 0.58$ max $\eta_p = 16.2$ at $\lambda = 9.26\,\mu$m	Na	$2\omega_1 + \omega_{IR}$ (2PR, 3PR)	YAG/OPO (20 ns, 3 kW) + CO (dye, 5 mW)	3
10.8	0.268	$\eta_q = 0.65$, $\eta_p = 26.4$	Na	$\omega_k + \omega_2 + \omega_{IR}$ (2PR, 3PR)	YAG/dye (ω_k:5.5 kW) + YAG ($\omega_2 = 2\omega$:20 kW) + CO_2 continuous, 7.5 mW)	4
10.8	0.268	$\eta_p = 0.09$	Na	$\omega_k + \omega_2 + \omega_{IR}$ (2PR, 3PR)	continuous Ar^+/dye (ω_k:0.3 W) + Ar^+ (ω_2:0.33 W) + CO_2 (0.3 mW)	17
10.6	0.33	$\eta_p = 0.23$	Na	$2\omega_k + \omega_{IR}$ (2PR, 3PR)	YAG/dye + CO_2 (200 mW)	208
9.13–10.91	0.3	$\eta_p = 10^{-6}$–10^{-2}	K	$2\omega_k + \omega_{IR}$ (2PR)	dye (650 MW/cm^2) + CO_2 (ω_{IR})	209
5.2–5.9	0.3	$\eta_p = 10^{-6}$–10^{-4}	K	$2\omega_k + \omega_{IR}$ (2PR)	dye (200 MW/cm^2) + CO_2 (ω_{IR})	209
3.39	0.33	$\eta_p = 10^{-4}$	Na	$2\omega_k - \omega_{IR}$ (2PR)	YAG/dye (5 kW) + He–Ne (1 MW)	210
3.06–3.19	0.46	$\eta_p = 10^{-5}$ (imaging, resolution 5–100)	Cs	$\omega_1 + \omega_{IR} + \omega_2$ (complementary scheme) (2PR, 3PR)	YAG/dye (ω_1:2–5$\times 10^5$ W/cm^2) + OPO (ω_{IR}) + OPO(ω_2)	6
3	0.45	$\eta_p = 10^{-1}$	Cs	$2\omega + \omega_{IR}$ (3PR)	YAG (ω:800 MW/cm^2) + OPO (ω_{IR})	211
2.94	0.456	$\eta_p = 0.2$ (imaging, resolution 10^3)	Cs	$2\omega + \omega_{IR}$ (2PR, 3PR)	Nd:$La_2Be_2O_5$ (ω:100 ns, 8 kW) + OPO (ω_{IR})	5
2.94	0.456	$\eta_p = 0.32$ (imaging, resolution 1.6×10^4)	Cs	$2\omega + \omega_{IR}$ (2PR, 3PR)	Nd:$La_2Be_2O_5$ (ω:40 ns, 300 kW, 275 kW/cm^2 + OPO (20 ns)	6
2.55–2.85	0.4	$\eta_q = 0.23$, $\eta_p \sim 1.5$	K	$\omega_1 - \omega_c + \omega_{IR}$ RS	YAG/dye (5 ns, mJ)	7
2.2	0.3	$\eta_q = 0.4$, $\eta_p = 1.2$	Na	$\omega_1 + \omega + \omega_{IR}$ (2PR, 3PR)	dye (ω_1:230 W) + YAG (ω:60 W) + OPO (ω_{IR}:10 W)	212
1.15	0.378	$\eta_p = 2\times 10^{-3}$	Tl	$2\omega_k - \omega_{IR}$ (2PR)	YAG/dye (20 kW) + (10 mW)	224
1.06	0.418	$\eta_p = 2\times 10^{-2}$	Ca	$2\omega_k - \omega_{IR}$ (2PR)	YAG/dye (15 ns, 10 kW) + YAG (continuous 0.1 W)	213
1.064, 1.061	0.61	$\eta_p = 0.01$	Na	$\omega_1 + \omega_{IR} + \omega_2$ (2PR, 3PR) complementary scheme	YAG/dye (ω_1:100 W) + YAG (ω_{IR}) + OPO (ω_2:50 W)	137a
1.06	0.323	$\eta_q = 0.12$, $\eta_p = 0.4$	Rb	$\omega_1 + \omega_{IR} + \omega_2$ complementary scheme	Rubin/dye (ω_1:20 ns, 22 kW) + YAG (120 mW) + dye	138
1.06	0.61	$\eta_p = 0.3$	Na	$\omega_{IR} + \omega_k - \omega_{IR}$ (2PR)	YAG (ω_{IR}) + dye (ω_k)	141

hundred cm^{-1}), with its absorption lines—again using metallic vapor. The quantum CF of converting IR spectra into the visible was 23%. It should be noted that the spectra are obtained in real time after but a single pump pulse. This arrangement holds promise for the detection of pico and femtosecond pulses. The frequency mixing method as a means of upconverting images and spectrographs of cosmic IR sources was discussed in Ref. 140. Wavefront reversal with IR conversion to the visible in Na vapor was carried out in Ref. 141: the power CF reached 30% with 13 lines/mm resolution. The main results of weak IR signal conversion studies in metallic vapors are collected in Table V.

Thus, we can employ resonance and quasiresonance nonlinear processes in metallic vapors to upconvert some IR radiation frequences with efficiencies exceeding those possible in nonlinear crystals (the maximum pulsed regime quantum CF in crystals for 10 micron radiation without the use of a resonator was 40% [142]). At the same time, by using the metallic vapors we lower pump power requirements, simplify signal filtering and lower the cost of the devices. We can also upconvert various IR frequencies into fixed visible and UV frequencies and transform wide IR frequency bands into visible or UV ranges while preserving the bandwidth. Further experimental and theoretical research is necessary to fully realize these advantages and possibilities.

8. WAVEFRONT REVERSAL

Radiation wavefront reversal (WR) has found extremely wide application in wavefront correction and control over the spatial characteristics of laser radiation (see, for example, Refs. 8, 143). WR consists of generating an electromagnetic wave whose phase is opposite in sign (complex-conjugate) to the generation (probe) wave at every point in space. Usually the frequency of the reversed wave equals or approximately equals that of the probe wave, but the two propagate in opposite directions. For example, if the probe wave is a spherical wave emitted from some point with radius of curvature R, the reversed wave is also spherical with radius of curvature R converging to that same point.

Formally radiation WR consists of complex conjugating the complex spatial amplitude component of a wave. The sign change in the phase in the course of phase-conjugated reflection eliminates phase distortion when the conjugation wave propagates throught the distorting medium in reverse.

In a medium with cubic nonlinearities the phase-conjugate wave (reverse wave) arises, for example, because of nonlinear polarization

$$P^{(3)} = \frac{N}{4}\chi^{(3)}A_1A_2A_3^*.$$

If $\omega_1 = \omega_2 = \omega_3$, $\mathbf{k}_1 = -\mathbf{k}_2$, the polarization wave will propagate with wave vector $-\mathbf{k}_3$ and phase that is the conjugate of A_3. In this case the generated wave can be expressed as $A_4 = RA_3^*$, where R is the nonlinear phase-conjugate reflection coefficient.

A large number of original research papers,[144] as well as a number of review papers (for example Ref. 8), have addressed the various features of WR and its applications. In particular, GNM are widely used for WR.

Wavefront reversal has been experimentally observed in the IR ($\lambda = 10.6\,\mu$m), visible, and UV spectral ranges, in both pulsed and continuous wave regimes, by using atomic and molecular gaseous media in resonace or nonresonance conditions. Various features and characteristics of WR in gaseous media are discussed in sufficient detail by one of the review papers on the subject.[8] It should be emphasized that gaseous media permit one to attain WR with significant (more than 1500%) gain.[145] Employing single photon resonances sharply enhances nonlinear susceptibilities and simultaneously reduced requirements for pumping intensity. In this way Lind and Steel[146] achieved WR of a c.w. dye laser, excited by Ar^+ laser in Na vapor, with reflection coefficient (RC) of 150%. This advance was used to construct a phase-conjugating mirror inside a c.w. laser resonator. In the above-cited paper[141] the authors investigated the WR characteristics of an IR signal converted into the red spectral range using Na vapor.

Research into the WR of CO_2 laser radiation in GNM occupies an important place among the studies of adaptive optics. In Ref. 9 SF_6 molecular gas was used to attain a CF$\approx$220% for the P(12) line ($\lambda = 10.51\,\mu$m) of a pulsed CO_2 laser. Infrared images destroyed by randomly inhomogenous media were reconstructed at the wavelength;[143] the initial, destroyed, and reconstructed beam images were visualized by thermomagnetic recording on amorphous magnetic films (see Fig. 23). Nonlinear optical processes giving rise to WR also found application in spectroscopic research (see, for example, Ref. 8), particularly in Doppler-free spectroscopy, occasionally with nonmonochromatic laser sources.

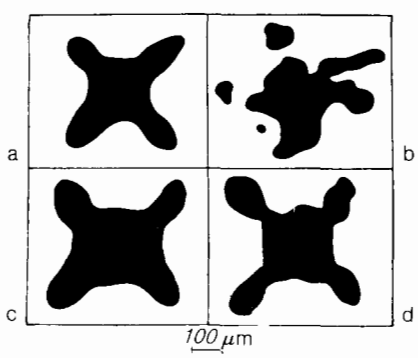

FIG. 23. Photograph of an IR image of an amplitude transparency in the signal (incident) (a,b) and reversed (c,d) beams.[147] a—Transparency image. (b)—Transparency image destroyed by a phase plate. c—Transparency image in the reversed wave, no phase plate. d—Reconstructed transparency image with phase plate.

9. CONCLUSION

The properties of individual atoms and molecules are best revealed in gaseous media. Those same media exhibit the sharpest resonance nonlinear optical response. The study of nonlinear optical properties of gases and molecules is one of the fascinating fields of physics, intimately connected with laser physics, nonlinear spectroscopy, and nonlinear optics. Atoms and molecules subjected to a strong spectroscopy, and nonlinear optics. Atoms and molecules subjected to a strong resonance laser field form a helpful model for research into strongly nonlinear processes—a field of physics in which a number of fundamental results were established in recent years.

On the other hand, nonlinear optical response of atoms and molecules in gaseous media provides unique opportunities of obtaining electromagnetic radiation with desirable properties, like tunable coherent VUV and SX radiation; controlling the phase of light oscillations in wavefront reversal schemes; converting light pulses of high energy, power, and aperture; improving the technology of generating and detecting IR radiation. The theoretical and technical understanding gained in the course of microscopic and macroscopic research into nonlinear optical processes in gases and vapors of chemical elements has contributed to the solution of many important scientific and technical problems.

In the various sections of this review we cite examples of these advances. Thus high resolution GNM-based VUV spectrometers, available to ordinary research laboratories and able, in some cases, to replace synchrotron sources, have markedly enriched and enhanced the research opportunities in spectroscopy of highly excited states of matter. Fairly simple nonlinear optical devices based on gases and metallic vapors have led to the development and perfection of qualitatively new methods in IR and adaptive optics. These advances will stimulate further development of fundamental and applied research in related scientific and technical fields—high-temperature plasma physics, chemistry, biology, and microtechnology—as well as in the field of nonlinear optics and nonlinear spectroscopy of atomic and molecular media.

APPENDIX

Interaction of intense laser radiation with resonance media. Limiting processes

In section 2 we discussed only the main optical processes that determine frequency conversion in GNM. As noted earlier, a distinctive feature of nonlinear optics is that an intense laser field usually stimulates a number of simultaneous linear and nonlinear processes with markedly different effects on frequency conversion. All these processes should be taken into account when optimal conversion conditions are selected. Let us consider some of these processes.

a) Single photon absorption and refraction.

Unperturbed linear absorption $\alpha_l(\omega_j)$ and refraction

$n_l(\omega_j)$ coefficients at field frequencies, as well as their modification by nonlinear processes in strong fields, can be calculated from the following expressions:

$$\alpha_l(\omega_j) = 4\pi\omega_j N c^{-1} \operatorname{Im}\chi^{(1)}(\omega_j) = N\sigma_l(\omega_j)$$
$$= 4\pi N(c\hbar)^{-1}\sum_m \omega_{mg}|d_{gm}|^2\Phi_{mg}(\omega_j)\Gamma_{mg}^{-1}$$
$$= N\sum_m 2r_e f_{gm}\Gamma_{mg}^{-1}\Phi_{mg}(\omega_j), \qquad (A1)$$

where σ_l is linear absorption cross-section, f_{gm} is the oscillator strength for the g–m transition, $r_e = e^2/mc^2 = 2.818\cdot10^{-13}$ cm, Φ_{mg} is the transition form factor which, for Lorentz-broadened transitions or frequency separations significantly exceeding Doppler broadening, has the form

$$\Phi_{mg}(\omega_j) = (2\Gamma_{mg}\omega_j)^2[(\omega_j^2-\omega_{mg}^2)^{-2}+(2\Gamma_{mg}\omega_j)^2]^{-1}, \qquad (A2)$$
$$n_l(\omega_j) = 1 - 2\pi N \operatorname{Re}\chi^{(1)}(\omega_j)$$
$$= 1 - 4\pi N\hbar^{-1}\sum_m \omega_{mg}|d_{gm}|^2(\omega_j^2-\omega_{mg}^2)^{-1}$$
$$= 1 - 2\pi c^2 r_e N\sum_m f_{gm}(\omega_j^2-\omega_{mg}^2)^{-1}. \qquad (A3)$$

b) Nonlinear absorption and refraction.

Nonlinear additions to absorption and refraction coefficients, for example, at frequency ω_2 when subjected to intense radiation at ω_1 are described by the following expressions respectively:

$$\delta\alpha_{nl}(\omega_2) = (\pi\omega_2 c^{-1}N|A_1|^2\operatorname{Im}\chi^{(3)}(\omega_2=\omega_1+\omega_2-\omega_1), \qquad (A4)$$
$$\delta n_{nl}(\omega_2) = -\frac{1}{2}\pi N|A_1|^2\operatorname{Re}\chi^{(3)}(\omega_2=\omega_1+\omega_2-\omega_1), \qquad (A5)$$
$$\chi^{(3)}(\omega_2) = \frac{1}{4\hbar^3}\Big|\sum_{\substack{m,\\ k=1,2}} d_{gm}d_{mn}(\omega_k-\omega_{mg})^{-2}\Big|^2$$
$$(\omega_1+\omega_2-\omega_{ng}-i\Gamma_{ng})^{-1}. \qquad (A6)$$

If the Doppler broadening of the two-photon resonance exceeds the collision broadening, expression (A6) must be averaged over the velocities.

Absorption of radiation frequently emerges as the principal effect which invalidates the applicability of the given-field approximation, while nonlinear corrections to the refraction coefficient lead to self-focusing and self-bending of beams of radiation and can exert a significant influence on wave synchronism. In a number of cases nonlinear refraction can turn out to be the principal limiting factor requiring compensation (cf., for example, Ref. 80).

c) Population shifts and the dynamical Stark effect.

The formulae (A4–A6) evaluate the effect of a strong field on the medium to the lowest order of perturbation theory. A more accurate calculation is usually hindered by spatial and temporal inhomogeneities of the fields. In many cases, when the first order approximations no longer hold, the effect of a strong field can be roughly estimated by replacing the particle density with saturated population differences of a resonance n-photon transition. If there exist several resonance transitions, the population of excited levels can qualitatively alter the expression for nonlinear susceptibility (see, for example, chapter 6 of Ref. 223).

Moreover, one should take into account modifications to resonance denominators in expressions for effective susceptibilities in the presence for a strong field. These modifications can be evaluated using the expression for the energy shift $\Delta\mathscr{E}_n$ of an energy level in a strong field E at frequency ω:

$$\Delta\mathscr{E}_n = \frac{1}{4}\sum_k\left(\frac{|d_{kn}E|^2}{\mathscr{E}_n-\mathscr{E}_k-\hbar\omega}+\frac{|d_{kn}E|^2}{\mathscr{E}_n-\mathscr{E}_k+\hbar\omega}\right). \qquad (A7)$$

Here we assume that single photon transition frequency separations are much larger than transition widths.

d) Multiphoton ionization and breakdown.

Multiphoton ionization depletes the interaction region of resonance atoms, and shifts and broadens energy levels. The relative contribution of ionization compared to other nonlinear processes depends on the order of the multiphoton ionization process.[218,219] For single photon ionization the ion density is described by the expression

$$N_i = N_n\left[1-\exp\left(-\frac{1}{2}\sigma_n\Phi\right)\right], \qquad (A8)$$

where N_n is the population of level n where the single photon ionization originates, σ_n is the cross section, and Φ is the density of radiated energy.

The constants of ionization broadening γ_{nn} and δ_{nn} can be evaluated from the following formulae:[47,219]

$$\gamma_{nn}(\varepsilon_0) = \pi\hbar|V_{n\varepsilon_0}|^2|_{\varepsilon_0=\mathscr{E}_n+\hbar\omega} \approx \sigma_n I(2\hbar\omega)^{-1},$$
$$\delta_{nn} = \pi^{-1}\int\gamma_{nn}(\varepsilon)(\varepsilon_0-\varepsilon)^{-1}\,d\varepsilon, \qquad (A9)$$

where $V_{n\varepsilon_0}$ is the matrix element of the Hamiltonian interaction corresponding to the transition from a discrete level n to the continuum state ε_0, I is the density of the radiated power.

At laser intensities exceeding some critical value E_c the material suffers optical breakdown.[220] In the case of weakly focused optical radiation delivered in pulses of nanosecond scale duration τ, E_c can be estimated from the formula

$$E_c \approx [10^{23}(N\tau)^{-1}]^{1/2}; \qquad (A10)$$

where N is the density (in atoms/cm^3), τ is in seconds, and E_c in V/cm.

Alongside the depletion of resonance atoms due to the appearance of the electronic component the refraction coefficients also change. The electronic contribution to the refraction coefficient is described by the expression

$$\Delta n = -2\pi N_e e^2(m_e\omega^2)^{-1}, \qquad (A11)$$

where N_e is the concentration, e and m_e are the electron charge and mass.

Ionization can destroy the central symmetry of the medium and allow even harmonic generation. In this way resonance generation of higher order even harmonics was achieved,[64] including eighth harmonic generation in the VUV range.[65]

e) Parametric brightening.

Another phenomenon which can have significant effect on nonlinear radiation conversion is parametric brightening due to interference of nonlinear processes (see, for example, Refs. 29, 138). The physical essence of this phenomenon can be illustrated by the example of resonace two-photon sum frequency generation $\omega_s = \omega_1+\omega_2+\omega_3(\omega_1+\omega_2=\omega_s-\omega_3\approx\omega_{ng})$. The off-diagonal density matrix element ρ_{ng} which describes both the two-photon excitation processes and the nonlinear susceptibility for the sum frequency gener-

ation process obeys the following equation in the interaction representation:

$$\left[\frac{\partial}{\partial t}+(\gamma_2-i\Omega)\right]\rho_{ng}$$
$$=in\left[r_1A_1A_2+r_2A_3^*A_s\exp\left(-i\Delta kz\right)\right], \qquad \text{(A12)}$$

Here Ω and γ_2 are the detuning and broadening of the two-photon resonance on the field-perturbed n–g transition, n is the population difference of n and g levels, r_1 is the compound matrix element for the n–g transition absorbing two photons, r_2 is the matrix element for a Raman scattering transition, and A_i are the slowly varying field amplitudes at frequencies ω_i.

It is apparent from (A12) that if, for example, the initial fields A_1 and A_3 are strong, whereas A_2 is weak, then as the A_s wave builds up the square-bracketed expression in (A12) will reduce to zero at some point in the medium. This implies that the polarizations induced by two-photon absorption and Raman scattering become equal in magnitude and opposite in sign. If $\Delta k=0$ both nonlinear absorption and nonlinear frequency conversion cease thereafter. The authors of Ref. 138 studied IR conversion in rubidium vapors and demonstrated that in the case of plane waves, no matter how long the nonlinear medium, this phenomenon ensures that only 50% of $\hbar\omega_2$ photons will be absorbed by two-photon processes, 25% will be converted to ω_s, and the remaining 25% will pass through the medium without interacting.

Parametric broadening was studied experimentally in Ref. 221; the theory of this phenomenon can be found in Refs. 29, 222.

In this appendix we have cited expressions that make it possible to estimate the circumstances in which the contribution of each of the competing processes becomes significant. The entire range of these processes should be considered in order to determine the ultimate efficiency of frequency conversion. Since the problem cannot in general be solved in closed form, each particular case requires a separate approach. Sample solutions of similar problems are available in Refs. 75, 78, 90, 219.

[1]D. M. Bloom *et al.*, Appl. Phys. Lett. **26**, 687 (1975).
[2]D. C. Hanna, M. A. Yuratich, and D. Cotter, *Nonlinear Optics of Free Atoms and Molecules*, Springer-Verlag, Berlin, 1979.
[3]D. M. Bloom *et al.*, Appl. Phys. Lett. **24**, 427 (1974).
[4]N. P. Makarov, A. K. Popov, and V. P. Timofeev, Appl. Phys. B **30**, 53 (1983); Kvantovaya Elektron. (Moscow) **10**, 664 (1983) [Sov. J. Quantum Electron. **13**, 408 (1983)].
[5]E. A. Stappaerts, S. E. Harris, and J. F. Young, Appl. Phys. Lett. **29**, 669 (1976).
[6]J. H. Newton and J. F. Young, IEEE J. Quantum Electron. **QE-16**, 268 (1980).
[7]D. S. Bethune *et al.*, Opt. Lett. **4**, 103 (1979); IBM J. Res. Dev. **23**, 23, 556 (1979); J. Chem. Phys. **74**, 2304 (1981); J. Chem. Phys. **75**, 2231 (1981).
[8]D. Pepper, Opt. Eng. **21**, 155 (1982).
[9]L. T. Bolotskikh and A. K. Popov, Appl. Phys. B **31**, 191 (1983).
[10]J. Reintjes, Appl. Opt. **19**, 3889 (1980).
[11]W. Jamros and B. P. Stoicheff, in: *Progress in Optics, Vol. 20*, edited by E. Wolf, North-Holland, Amsterdam, 1983, p. 325.
[12]R. Wallenstein, Laser und Optoelektron. **3**, 29 (1982); Izv. Akad. Nauk SSSR, Ser. Fiz. **50**, 614 (1986) [Bull. Acad. Sci. USSR, Phys. Ser. **50**, No. 3, 185 (1986)].
[13]H. Egger, H. Pummer, and C. K. Rhodes, Laser Focus **18**, 64 (1984).
[14]J. Bokor, P. H. Buchsbaum, and R. R. Freeman, Opt. Lett. **8**, 217 (1983).
[15]M. Rowekamp, H. F. Dobele, and B. Rückle, IEEE J. Quantum Electron. **QE-20**, 1284 (1984).
[16]V. F. Lukinykh *et al.*, Appl. Phys. B **34**, 171 (1984).
[17]V. G. Arkhipkin, A. L. Vysotin, Im Thek-de *et al.*, Kvant. Elektron. **13**, 1352 (1986) [Sov. J. Quantum Electron. **16**, 888 (1986)].
[18]S. C. Wallace, in: *Photoselective Chemistry, Part 2*, edited by J. Jortner, R. D. Levine, and S. A. Rice, Wiley, New York, 1981, p. 135.
[19]B. P. Stoicheff *et al.*, in: *Laser Techniques for Extreme Ultraviolet Spectroscopy*, eds. T. J. McIlrath and R. R. Freeman, Am. Inst. Phys., N.Y., 1982, p. 19.
[20]M. D. Rotschild *et al.*, Phys. Rev. A **23**, 206 (1981).
[21]J. E. Rothenberg, J. F. Young, and S. E. Harris, Opt. Lett. **6**, 363 (1981).
[22]J. C. Miller, R. N. Compton, and C. D. Cooper, J. Chem. Phys. **76**, 3967 (1982).
[23]a) R. W. Dreyfus, P. Bogen, and H. Langer, in: *Laser Techniques for Extreme Ultraviolet Spectroscopy*, eds. T. J. McIlrath and R. R. Freeman, Am. Inst. Phys., N.Y., 1982, p. 57. b) K. G. H. Baldwin, J. P. Marados, and D. D. Burgess, J. Phys. D **17**, 169 (1984).
[24]C. K. Rhodes, in: *Novel Materials and Technology in Condensed Matter*, edited by G. W. Grabtree and P. Vashishta, Elsevier Science, New York, 1982, p. 151.
[25]G. C. Bjorklund, S. E. Harris, and J. F. Young, Appl. Phys. Lett. **25**, 451 (1974).
[26]M. E. Movsesyan, V. A. Iradyan, and I. N. Badalyan, Pis'ma Zh. Eksp. Teor. Fiz. **6**, 631 (1967) [JETP Lett. **6**, 127 (1967)]. P. P. Sorokin *et al.*, Appl. Phys. Lett. **10**, 44 (1967). J. M. Rokni and S. Yatsiv, IEEE J. Quantum Electron. **QE-3**, 329 (1967). O. J. Lumpkin, IEEE J. Quantum Electron. **QE-4**, 226 (1968). V. M. Arutyunyan, Zh. Eksp. Teor. Fiz. **58**, 37 (1970) [Sov. Phys. JETP **31**, 22 (1970)]. Yu. M. Kirin and S. G. Rautian, Pis'ma Zh. Eksp. Teor. Fiz. **11**, 340 (1970) [JETP Lett. **11**, 226 (1970)]. A. M. Bonch-Bruevich *et al.*, Pis'ma Zh. Eksp. Teor. Fiz. **11**, 431 (1970) [JETP Lett. **11**, 290 (1970)]. F. A. Korolev, S. A. Bakhramov, and V. I. Odintsov, Pis'ma Zh. Eksp. Teor. Fiz. **12**, 131 (1970) [JETP Lett. **12**, 90 (1970)]. S. A. Akhmanov *et al.*, Pis'ma Zh. Eksp. Teor. Fiz. **15**, 186 (1972) [JETP Lett. **15**, 129 (1972)].
[27]T. Ya. Popova and A. K. Popov, Zh. Eksp. Teor. Filz. **52**, 1517 (1967) [Sov. Phys. JETP **25**, 1007 (1967)]. A. B. Budnitskiĭ and A. K. Popov, Opt. Specktrosk. **29**, 1032 (1970) [Opt. Spectrosc. (USSR) **29**, 550 (1970)]. A. K. Popov, V. I. Barantsov, and G. Kh. Tartakovskiĭ, *XII Urals Spectroscopy Conference* (in Russian, Inst. Fiz. Mat., Urals Nauchn. Tsentr Akad. Nauk SSSR, Sverdlovsk, 1971, Iss. 3, p. 49; *Abstracts of Papers Presented at XVII All-Union Spectroscopy Conference. "Laser Spectroscopy" Issue* (in Russian), Inst. Fiz., Akad. Nauk Beloruss. SSR, Minsk, 1971, p. 40.
[28]S. A. Akhmanov and R. V. Khokhlov, *Nonlinear Optics*, Gordon and Breach, N.Y., 1972. [Russ. original, VINITI, M., 1964]. M. Schubert and B. Wilhelmi, *Nonlinear Optics and Quantum Electronics*, Wiley, New York, 1986 [Russ. transl., Mir, M., 1973]. L. P. Rapoport, B. A. Zon, and N. L. Manakov, *Theory of Multiphoton Processes in Atoms* (in Russian), Atomizdat, M., 1978.
[29]*Resonance Interactions of Light with Matter* (in Russian), edited by V. S. Butylkin, A. E. Kaplan, Yu. G. Khronopulo, and E. I. Yakubovich, Nauka, M., 1977.
[30]B. J. Orr and J. F. Ward, Mol. Phys. **20**, 513 (1971).
[31]A. Yariv, IEEE J. Quantum Electron. **QE-13**, 943 (1977). T. K. Yee and T. K. Gustafson, Phys. Rev. A **18**, 1597 (1978). J. P. Uyemura, IEEE J. Quantum Electron. **QE-16**, 472 (1980). Y. Prior, IEEE J. Quantum Electron. **QE-20**, 37 (1984).
[32]H. Puel and C. R. Vidal, Phys. Rev. A **14**, 2225 (1976).
[33]D. Grischkowski, M. M. T. Loy, and P. F. Liao, Phys. Rev. A **12**, 2514 (1975).
[34]A. M. Afanas'ev and É. A. Manykin, Zh. Eksp. Teor. Fiz. **48**, 931 (1965) [Sov. Phys. JETP **21**, 619 (1965)].
[35]H. Eicher, IEEE J. Quantum Electron. **QE-11**, 121 (1975).
[36]J. F. Ward and G.-H. New, Phys. Rev. **185**, 57 (1969).
[37]G. C. Bjorklund, IEEE J. Quantum Electron. **QE-11**, 287 (1975).
[38]A. K. Popov and V. P. Timofeev, Opt. Commun. **20**, 94 (1977).
[39]V. G. Arkhipkin and A. K. Popov, *IR Radiation Conversion in Resonance Nonlinear Media* (in Russian), IFSO-150F Preprint, Krasnoyarsk, 1980.
[40]S. A. Akhmanov, in *Nonlinear Spectroscopy*, edited by N. Bloembergen, North-Holland, Amsterdam, 1977, p. 239 [Russ. transl., Mir, M., 1979, p. 322].
[41]I. V. Tomov and M. Richardson, IEEE J. Quantum Electron. **QE-12**, 521 (1976).
[42]A. N. Dubovik, a) Vestnik MGU, Ser. Fiz. Astron.: b) *Higher-Order Optical Nonlinearities and Multiphoton Processes in Isotropic Media* (in Russian), Candidate dissertation abstract, MGU, M., 1981.
[43]J. Reintjes, C.-Y. She, and R. C. Eckhardt, IEEE J. Quantum Electron. **QE-14**, 581 (1978).
[44]G. H. C. New, Opt. Commun. **38**, 189 (1981).
[45]U. Fano and J. W. Cooper, *Spectral Distribution of Atomic Oscillator Strengths*, Rev. Mod. Phys. **40**, 441 (1968) [Russ. transl., Nauka, M., 1972].

[46]J. Armstrong, in *Nonlinear Spectroscopy*, edited by N. Bloembergen, North-Holland, Amsterdam, 1977, p. 152. [Russ. transl., Mir, M., 1979, p. 192].
[47]Yu. I. Geller and A. K. Popov, *Laser Tuning of Nonlinear Resonances in Continuous Spectra* (in Russian), Nauka, Novosibirsk, 1981.
[48]M. Crance and L. Armstrong Jr., J. Phys. B **15**, 4637 (1982). G. Alber and P. Zoller, Phys. Rev. A **27**, 1373 (1983). G. S. Agarwal and P. A. Lakshmi, Phys. Rev. A **28**, 3430 (1983).
[49]T. R. Royt and Chi H. Lee, Appl. Phys. Lett. **30**, 332 (1977).
[50]G. S. Agarwal and S. L. Haan, Phys. Rev. A **29**, 2552, 2565 (1984).
[51]Yu. I. Geller and A. K. Popov, Phys. Lett. A **56**, 453 (1976).
[52]A. Lami and N. K. Rahman, Opt. Commun. **43**, 383 (1982); Phys. Rev. A **26**, 3360 (1982); J. Mol. Struct. **93**, 295 (1983).
[53]Yu. I. Geller and A. K. Popov, Zh. Eksp. Teor. Fiz. **78**, 506 (1980) [Sov. Phys. JETP **51**, 255 (1980)].
[54]Yu. I. Geller and A. K. Popov, Pis'ma Zh. Tekh. Filz. **6**, 151 (1980) [Sov. Tech. Phys. Lett. **6**, 67 (1980)]; Phys. Lett. A **82**, 4 (1981).
[55]S. S. Dimov *et al.*, Kvantovaya Elektron. (Moscow) **10**, 1635 (1983) [Sov. J. Quantum Electron. **13**, 1075 (1983)]; Appl. Phys. B **30**, 35 (1983).
[56]P. E. Coleman and P. L. Knight, Opt. Commun. **42**, 171 (1982); J. Phys. B **15**, L235 (1982). K. Rzazewski and J. H. Eberly, Phys. Rev. Lett. **47**, 408 (1981); J. Phys. B **15**, L661 (1982).
[57]T. Hänsch and P. Toschek, Z. Phys. **236**, 373 (1970).
[58]D. S. Bethune, R. W. Smith, and Y. R. Shen, Phys. Rev. A **17**, 277 (1978).
[59]D. J. Gauthier, J. Krasinski, and R. W. Boyd, Opt. Lett. **8**, 211 (1977).
[60]H. Uchiki, H. Nakatsuka, and M. Matsuoka, Phys. Rev. Lett. **38**, 894 (1977); Opt. Commun. **30**, 345 (1979).
[61]M. H. Dunn, Phys. Rev. Lett. **45**, 346 (1983).
[62]T. Mossberg, A. Flusberg, and S. R. Hartman, Phys. Rev. Lett. **25**, 121 (1978). K. Miyazaki, T. Sato, and H. Kashiwagi, Phys. Rev. A **23**, 1358 (1981). J. Okada, Y. Fukuda, and M. Matsuoka, J. Phys. Soc. Jpn. **50**, 1301 (1981). J. Bokor *et al.*, Opt. Lett. **6**, 182 (1981). W. Jamroz, P. E. Laroque, and B. P. Stoicheff, Opt. Lett. **7**, 148 (1982).
[63]V. G. Arkhipkin *et al.*, Opt. Quantum Electron. **13**, 436 (1981).
[64]V. A. Kiyashko *et al.*, Appl. Phys. B **35**, 53 (1985).
[65]A. S. Aleksandrovskiĭ *et al.*, *Generation of Coherent Vacuum-Ultraviolet Radiation in Higher-Order Nonlinear Processes* (in Russian), IFSO-347F Preprint, Krasnoyarsk, 1985.
[66]D. S. Bethune, Phys. Rev. A **23**, 3139 (1981); **25**, 2345 (Erratum) (1982).
[67]S. A. Bakhramov, G. Kh. Tartakovskiĭ, and P. K. Khabibulaev, *Nonlinear Resonance Processes and Frequency Conversion in Gases* (in Russian), Fan, Tashkent, 1981.
[68]S. A. Akhmanov, in *Nonlinear Spectroscopy*, edited by N. Bloembergen, North-Holland, Amsterdam, 1977, p. 255 [Russ. transl., Mir, M., 1979, p. 347].
[69]D. Cotter, D. C. Hanna, and R. Wyatt, Appl. Phys. **8**, 333 (1975).
[70]Y. R. Shen, in *Light Scattering in Solids*, edited by M. Cardona, Springer-Verlag, New York, 1975.
[71]J. J. Wynne and P. P. Sorokin, in *Nonlinear Infrared Generation*, edited by Y. R. Shen, Springer-Verlag, New York, 1977.
[72]S. E. Harris, Appl. Phys. Lett. **31**, 498 (1977); in: *Laser Techniques for Extreme Ultraviolet Spectroscopy*, eds. T. J. McIlrath and R. R. Freeman, Am. Inst. Phys., N.Y., 1982, p. 137.
[73]J. E. Rothenberg and S. E. Harris, IEEE J. Quantum Electron. **QE-17**, 418 (1984). R. G. Caro *et al.*, Appl. Phys. Lett. **42**, 9 (1983); Phys. Rev. A **30**, 1419 (1984). J. S. Helman *et al.*, Phys. Rev. A **27**, 562 (1982). A. E. Martirosyan and O. V. Papanyan, Kvantovaya Elektron. (Moscow) **10**, No. 1, 166 (1983) [Sov. J. Quantum Electron. **13**, No. 1, 99 (1983)]. J. C. White, IEEE J. Quantum Electron. **QE-20**, 185 (1984). K. Ludewigt, K. Birkman, and B. Wellegehansen, Appl. Phys. B **33**, 133 (1984).
[74]H. Pummer *et al.*, Phys. Rev. A **28**, 795 (1983). K. Boyer *et al.*, J. Opt. Soc. Amer. B **1**, 3 (19184).
[75]Yu. A Il'inskiĭ and V. D. Taranukhin, Kvantovaya Elektron. (Moscow) **2**, 1497 (1975) [Sov. J. Quantum Electron. **5**, 805 (1975)]. V. I. Anikin *et al.*, Kvantovaya Elektron. (Moscow) **3**, 330 (1976) [Sov. J. Quantum Electron. **6**, 174 (1976)]. A. T. Georges *et al.*, Phys. Rev. **15**, 300 (1977). E. A. Stappaerts, IEEE J. Quantum Electron. **QE-15**, 110 (1979). H. Scheingraber *et al.*, IEEE J. Quantum Electron. **QE-19**, 1747 (1983).
[76]C. R. Vidal, Appl. Opt. **19**, 3897 (1980).
[77]E. A. Stappaerts *et al.*, IEEE J. Quantum Electron. **QE-12**, 330 (1976). V. I. Anikin, S. A. Akhmanov *et al.*, Kvantovaya Elektron. (Moscow) **3**, 2014 (1976) [Sov. J. Quantum Electron. **6**, 1096 (1976)]. A. M. Steba and V. L. Strizhevskiĭ, Ukr. Fiz. Zh. **25**, 86 (1980) [Ukr. Phys. J. **25** (1980)].
[78]V. I. Anikin *et al.*, Zh. Eksp. Teor. Fiz. **72**, 1727 (1977) [Sov. Phys. JETP **45**, 906 (1977)]. J.-C. Diels *et al.*, Phys. Rev. A **19**, 1589 (1979). J. N. Elgin, J. Phys. B **13**, 3043 (1980).
[79]J. F. Ward and A. V. Smith, Phys. Rev. Lett. **35**, 653 (1975). C. C. Wang and L. I. Davis, Phys. Rev. Lett. **35**, 650 (1975).
[80]H. Puell and C. R. Vidal, Opt. Commun. **27**, 165 (1978). G. V. Mironov, A. K. Popov, and V. V. Slabko, Opt. Quantum. Electron. **17**, 435 (1985); Kvantovaya Elektron. (Moscow) **13**, 1138 (1986) [Sov. J. Quantum. Electron. **16**, 749 (1986)].
[81]G. C. Bjorklund *et al.*, Appl. Phys. Lett. **29**, 729 (1976).
[82]R. B. Miles and S. E. Harris, IEEE J. Quantum Electron **QE-9**, 470 (1973).
[83]C. R. Vidal and J. J. Cooper, J. Appl. Phys. **40**, 3370 (1969). C. R. Vidal and F. B. Haller, Rev. Sci. Instrum. **42**, 1770 (1971).
[84]M. K. Kodirov *et al.*, IFSO-221F Preprint (in Russian), Krasnoyarsk, 1982. A. S. Aleksandrovskiĭ *et al.*, IFSO-297F Preprint (in Russian), Krasnoyarsk, 1984.
[85]C. R. Vidal and M. M. Hessel, J. Appl. Phys. **43**, 2776 (1972).
[86]D. M. Bloom *et al.*, Appl. Phys. Lett. **27**, 390 (1975).
[87]H. Scheingraber and C. R. Vidal, Rev. Sci. Instrum. **52**, 1010 (1981).
[88]R. Hilbig and R. Wallenstein, IEEE J. Quantum Electron. **QE-19**, 1759 (1983).
[89]A. H. Kung, Opt. Lett. **8**, 24 (1983). C. T. Rettner *et al.*, J. Phys. Chem. **88**, 4459 (1984).
[90]L. Hellner and J. Lukasik, Opt. Commun. **51**, 347 (1984).
[91]R. R. Freeman *et al.*, Phys. Rev. A **26**, 3029 (1982).
[92]V. V. Lebedev, V. M. Plyasulya, B. I. Troshin *et al.*, Kvantovaya Elektron. (Moscow) **12**, 866 (1985) [Sov. J. Quantum Electron. **15**, 568 (1985)].
[93]V. F. Lukinykh, S. A. Myslivets, A. K. Popov *et al.*, Appl. Phys. B **38**, 143 (1985).
[94]V. G. Arkhipkin, Yu. I. Geller, A. K. Popov *et al.*, Kvantovaya Elektron. (Moscow) **12**, 1420 (1985) [Sov. J. Quantum Electron. **15**, 938 (1985)]. V. G. Arkhipkin, Yu. I. Geller, A. K. Popov *et al.*, Appl. Phys. B **38**, 93 (1985).
[95]V. K. Popov, Usp. Fiz. Nauk **147**, 587 (1985) [Sov. Phys. Usp. **28**, 1031 (1985)].
[96]V. G. Arkhipkin and A. K. Popov, IFSO-300-302F Preprints, (In Russian) Krasnoyarsk, 1984.
[97]V. V. Slabko, A. K. Popov, and V. F. Lukinykh, Pis'ma Zh. Tekh. Fiz. **3**, 1263 (1977) [Sov. Tech. Phys. Lett. **3**, 522 (1977)].
[98]T. J. McIlrath, in: *Laser Techniques for Extreme Ultraviolet Spectroscopy*, eds. T. J. McIlrath and R. R. Freemen, Am. Inst. Phys., N.Y., 1982, p. 9.
[99]J. A. Armstrong and J. J. Wynne, Phys. Rev. Lett. **39**, 1483 (1974).
[100]A. S. Provorov *et al.*, J. Chem. Phys. **68**, 5393 (1977).
[101]S. V. Filsth, R. Wallenstein, and H. Zacharias, Opt. Commun. **23**, 231 (1977); Phys. Rev. Lett. **39**, 1138 (1977).
[102]C. R. Vidal, in: *Laser Techniques for Extreme Ultraviolet Spectroscopy*, eds. T. J. McIlrath and R. R. Freeman, Am. Inst. Phys., N.Y., 1982, p. 431. P. Klopotek and C. R. Vidal, J. Opt. Soc. Am. B **2**, 869 (1985); Can. J. Phys. **62**, 1426 (1984).
[103]R. Wallenstein, Opt. Commun. **33**, 119 (1980).
[104]E. E. Marinero *et al.*, Chem. Phys. Lett. **95**, 486 (1983).
[105]T. Srinivasan *et al.*, IEEE J. Quantum Electron. **QE-19**, 1270 (1983).
[106]A. N. Zaidel', *Atomic Fluorescence Analysis* (in Russian), Nauka, M., 1980.
[107]R. Mahon and Y. M. Yiu, Opt. Lett. **5**, 279 (1980).
[108]H. Zacharias *et al.*, Opt. Commun. **35**, 185 (1980); **37**, 15 (1981). H. Rottke *et al.*, in: *Laser Techniques for Extreme Ultraviolet Spectroscopy*, eds. T. J. McIlrath and R. R. Freeman, Am. Inst. Phys., N.Y., 1982. H. Rottke and K. H. Welge, Preprint, FRG, 1982.
[109]S. C. Wallace and K. K. Innes, J. Chem. Phys. **72**, 4805 (1980).
[110]K. N. Drabovich, A. N. Dubovnik, and A. A. Surovegin, Izv. Akad. Nauk SSSR, Ser. Fiz. **42**, 2580 (1978) [Bull. Acad. Sci. USSR, Phys. Ser. **42**, No. 12, 98 (1978)]. K. N. Drabovich *et al.*, Izv. Akad. Nauk SSSR, Ser. Fiz. **46**, 1637 (1982) [Bull. Acad. Sci. USSR, Phys. Ser. **46**, No. 8, 180 (1982)].
[111]Yu. I. Geller and E. V. Timchenko, Opt. Spektrosk. **57**, 701 (1984) [Opt. Spectrosc. (USSR) **57**, 425 (1984)].
[112]K. Jain *et al.*, IBM J. Res. Dev. **26**, 151 (1982).
[113]C. K. Rhodes, *Laser Interaction and Related Phenomena, Vol. 6*, Plenum Press, New York, 1984, p. 87.
[114]V. N. Smiley, Adv. Electron. Electron Phys. **56**, 1 (1981).
[115]N. Djen and R. Burnham, Appl. Phys. Lett. **30**, 473 (1977).
[116]S. J. Brosnan *et al.*, Opt. Lett. **7**, 154 (1982).
[117]T. Loree *et al.*, IEEE J. Quantum Electron. **QE-15**, 337 (1979).
[118]H. Komine *et al.*, Appl. Phys. Lett. **40**, 551 (1982).
[119]J. R. Murray *et al.*, IEEE J. Quantum Electron. **QE-15**, 342 (1979).
[120]D. Cotter and D. C. Hanna, Opt. Quantum Electron. **9**, 509 (1977).
[121]D. Cotter, D. C. Hanna, and R. Wyatt, Opt. Commun. **16**, 256 (1976).
[122]R. T. V. Kung and I. Itzkan, Appl. Phys. Lett. **29**, 780 (1976).
[123]D. R. Grischkowski, P. P. Sorokin, and J. R. Lankard, Opt. Commun.

18, 205 (1976).
[124]P. P. Sorokin and J. R. Lankard, IEEE J. Quantum Electron. **QE-9**, 227 (1973).
[125]R. Wyatt and D. Cotter, Opt. Commun. **32**, 481 (1980).
[126]P. P. Sorokin *et al.*, in: *Laser Spectroscopy*, eds. R. C. Brewer and A. Mooradian, Plenum Press, N.Y., 1974, p. 103.
[127]W. R. Trutna and R. L. Byer, Appl. Opt. **19**, 301 (1980); A. Berry *et al.*, Opt. Commun. **43**, 229 (1982).
[128]A. De Martino, R. Frey, and F. Pradere, IEEE J. Quantum Electron. **QE-16**, 1184 (1980).
[129]S. J. Brosnan *et al.*, Appl. Phys. Lett. **30**, 330 (1977).
[130]L. T. Bolotskikh and A. K. Popov, Avtometria No. 6, 61 (1978).
[131]S. R. Brueck and H. Kildal, Appl. Phys. Lett. **33**, 928 (1978).
[132]S. A. Akhmanov *et al.*, Pis'ma Zh. Tekh. Fiz. **5**, 1504 (1979) [Sov. Tech. Phys. Lett. **5**, 638 (1979)].
[133]A. D. May *et al.*, Can. J. Phys. **48**, 2331 (1970).
[134]S. R. Brueck and H. Kildal, *Laser and Its Applications*, Springer-Verlag, N.Y., 1981, p. 147.
[135]K. M. Chung *et al.*, IEEE J. Quantum Electron. **QE-15**, 874 (1979). S. S. Alimpiev *et al.*, Kratk. Soobshch. Fiz. (FIAN) No. 9, 3 (1982) [Sov. Phys. Lebedev Inst. Rep. No. 9, 1 (1982)]. V. N. Varakin and V. M. Gordienko, Kvantovaya Elektron. (Moscow) **9**, 1941 (1982) [Sov. J. Quantum Electron. **12**, 1265 (1982)].
[136]É. S. Voronin and V. L. Strizhevskii, Usp. Fiz. Nauk **127**, 99 (1979) [Sov. Phys. Usp. **22**, 26 (1979)].
[137]a) S. A. Komarov *et al.*, Kvantovaya Elektron. (Moscow) **7**, 2485 (1980) [Sov. J. Quantum Electron. **10**, 1449 (1980)]. b) V. G. Arkhipkin and A. K. Popov, Pis'ma Zh. Tekh. Fiz. **7**, 414 (1981) [Sov. Tech. Phys. Lett. **7**, 176 (1981)].
[138]V. A. Kiyashko *et al.*, Appl. Phys. B **30**, 157 (1983).
[139]K. S. Krishnan, J. S. Ostrem, and E. A. Stappaerts, Opt. Eng. **17**, 108 (1978).
[140]J. Falk, Laser Focus **15**, 73 (1979).
[141]V. V. Krasnikov *et al.*, Kvantovaya Elektron. (Moscow) **10**, 1502 (1983) [Sov. J. Quantum Electron. **13**, 983 (1983)].
[142]W. Lantz and P. Koidl, Appl. Phys. Lett. **31**, 99 (1977).
[143]B. Ya. Zel'dovich, N. F. Pilipetskii, and V. V. Shkunov, *Principles of Phase Conjugation*, Springer-Verlag, New York, 1985.
[144]Quantum Electronics: Bibliographical Reference (in Russian), Inst. Fiz., Akad. Nauk Beloruss. SSR, Minsk, 1986.
[145]D. M. Bloom *et al.*, Opt. Lett. **3**, 58 (1978).
[146]R. C. Lind and D. G. Steel, Opt. Lett. **6**, 554 (1981).
[147]K. S. Aleksandrov, L. T. Bolotskikh, A. K. Popov *et al.*, Dokl. Akad. Nauk SSSR **286**, 610 (1986) [Sov. Phys. Dokl. **31**, 57 (1986)].
[148]R. Hilbig and R. Wallenstein, Appl. Opt. **21**, 913 (1982).
[149]A. H. Kung, Appl. Phys. Lett. **25**, 653 (1974).
[150]R. Hilbig and R. Wallenstein, IEEE J. Quantum Electron. **QE-17**, 1566 (1981).
[151]D. Cotter, Opt. Commun. **31**, 391 (1979).
[152]R. Wallenstein, Opt. Commun. **33**, 119 (1980).
[153]H. Langer, H. Puell, and H. Röhr, Opt. Commun. **34**, 137 (1980).
[154]R. Mahon, T. J. McIlrath, and D. W. Koopman, Appl. Phys. Lett. **33**, 305 (1978).
[155]R. Mahon and Y. M. Yiu, Opt. Lett. **5**, 279 (1980).
[156]S. A. Batishche, V. S. Burakov, V. I. Gladushchak *et al.*, Pis'ma Zh. Tekh. Fiz. **8**, 1375 (1986) [Sov. Tech. Phys. Lett. **8**, 591 (1986)].
[157]R. A. Ganeev, I. A. Kulagin, T. Usmanov *et al.*, Kvantovaya Elektron. (Moscow) **9**, 2508 (1982) [Sov. J. Quantum Electron. **12**, 1637 (1982)].
[158]D. Cotter, Opt. Lett. **4**, 134 (1979).
[159]W. Zapka, D. Cotter, and U. Brackmann, Opt. Commun. **36**, 79 (1982).
[160]J. Reintjes, Opt. Lett. **4**, 242 (1979); **5**, 342 (1980).
[161]B. I. Troshin, A. A. Chernenko, and V. P. Chebotaev, Zh. Tekh. Fiz. **52**, 2422 (1982) [Sov. Phys. Tech. Phys. **27**, 1494 (1982)].
[162]R. Hilbig and R. Wallenstein, Opt. Commun. **44**, 283 (1983).
[163]E. E. Marinero, Ch. T. Rettner, R. N. Zare *et al.*, Chem. Phys. Lett. **95**, 486 (1983).
[164]S. E. Harris, J. F. Young, A. H. Kung *et al.*, *Laser Applications in Optics and Spectroscopy, Vol. 2*, Addison Wesley, Mass., 1975, p. 181.
[165]R. Hilbig, A. Lago, and R. Wallenstein, Opt. Commun. **49**, 297 (1984).
[166]H. Pummer, T. Strinivasan, H. Egger *et al.*, Opt. Lett. **7**, 93 (1982).
[167]R. Hilbig and R. Wallenstein, IEEE J. Quantum Electron. **QE-19**, 194 (1983).
[168]J. Hager and S. C. Wallace, Chem. Phys. Lett. **90**, 472 (1982).
[169]A. I. Ferguson and E. G. Arthurs, Phys. Lett. A **58**, 298 (1976).
[170]J. R. Taylor, Opt. Commun. **18**, 504 (1976).
[171]T. R. Royt and Chi H. Lee, Appl. Phys. Lett. **30**, 332 (1977).
[172]R. T. Hodgson, P. P. Sorokin, and J. J. Wynne, Phys. Rev. Lett. **20**, 1183 (1974). P. P. Sorokin, J. J. Wynne, J. A. Armstrong *et al.*, Ann. N. Y. Acad. Sci **267**, 30 (1976).
[173]H. Scheingraber, H. Puel, and C. R. Vidal, Phys. Rev. A **18**, 1585 (1978).
[174]J. Bokor, R. R. Freeman, R. L. Panock *et al.*, Opt. Lett. **6**, 182 (1981).
[175]D. J. Bradley, in: *Ultrashort Light Pulses* (Ed.) S. L. Shapiro, Springer-Verlag, Berlin, 1977, p. 17 [Russ. transl., Mir, M., 1981, p. 35].
[176]R. R. Freeman, G. C. Bjorklund, N. P. Economou *et al.*, Appl. Phys. Lett. **33**, 731 (1978).
[177]G. A. Zdasiuk, M. Sc. Thesis, Univ. of Toronto, 1975.
[178]G. C. Bjorklund, J. E. Bjorkholm, R. R. Freeman *et al.*, Appl. Phys. Lett. **31**, 330 (1977).
[179]S. C. Wallace and G. A. Zdasiuk, Appl. Phys. Lett. **28**, 449 (1976).
[180]M. N. R. Hutchinson and R. J. Thomas, IEEE J. Quantum Electron. **QE-19**, 1823 (1983).
[181]J. Heinrich, K. Hollenberg, and W. Behmenburg, Appl. Phys. B **33**, 225 (1984).
[182]K. K. Innes, B. P. Stoicheff, and S. C. Wallace, Appl. Phys. Lett. **29**, 715 (1976).
[183]H. Junginger, H. P. Puell, H. Scheingraber *et al.*, IEEE J. Quantum Electron **QE-16**, 1132 (1980); **QE-17**, 557 (1981).
[184]A. Timmerman and R. Wallenstein, Opt. Lett. **8**, 517 (1983).
[185]F. Vallee, F. D. E. Rougemont, and J. Lukasik, IEEE J. Quantum Electron **QE-19**, 1332 (1983).
[186]W. Jamroz, P. E. Labocque, and B. P. Stoicheff, Opt. Lett. **7**, 617 (1982).
[187]T. J. McKee, B. P. Stoicheff, and S. C. Wallace, Opt. Lett. **3**, 207 (1978).X
[188]K. Miyazaki, H. Sakai, and T. Sato, Opt. Lett. **9**, 457 (1984).
[189]R. G. Caro, A. Gostela, and C. E. Webb, Opt. Lett. **6**, 464 (1981).
[190]R. Mahon and F. S. Tomkins, IEEE J. Quantum Electron **QE-18**, 913 (1982).
[191]Y. M. Yiu, K. D. Bonin, and T. J. McIlrath, Opt. Lett. **7**, 268 (1982).
[192]R. Mahon, T. J. McIlrath, F. S. Tomkins *et al.*, Opt. Lett. **4**, 260 (1979).
[193]F. S. Tomkins and R. Mahon, Opt. Lett. 7, 304 (1982).
[194]K. S. Hsu, A. H. Kung, L. J. Zych *et al.*, IEEE J. Quantum Electron **QE-12**, 60 (1976).
[195]M. L. Dlabal, J. Reintjes, and L. Tankersley, Proc. SPIE (Int. Soc. Opt. Eng.) **476**, 65 (1984).
[196]F. Vallee *et al.*, Opt. Commun. **42**, 148 (1982); **43**, 287 (1982).
[197]B. I. Troshn, V. P. Chebotaev, and A. A. Chernenko, Pis'ma Zh. Eksp. Teor. Fiz. **27**, 293 (1978) [JETP Lett. **27**, 273 (1978)].
[198]R. R. Freeman, R. M. Jopson, and J. Bokor, in: *Laser Techniques for Extreme Ultraviolet Spectroscopy*, eds. T. J. McIlrath and R. R. Freeman, Am. Inst. Phys., N.Y., 1982, p. 19.
[199]V. V. Slabko, A. K. Popov, and V. F. Lukinykh, Appl. Phys. **15**, 239 (1978).
[200]H. Egger, R. T. Hawkins, J. Bokor *et al.*, Opt. Lett. **5**, 282 (1980).
[201]D. J. Bradley, M. H. R. Hutchinson, and C. C. Lind, *Tunable Lasers and Applications*, Springer-Verlag, N.Y., p. 40.
[202]D. I. Metchkov, V. M. Mitev, L. I. Pavlov *et al.*, Opt. Commun. **21**, 391 (1977). V. L. Doitcheva, V. M. Mitev, L. I. Pavlov *et al.*, Opt. Quantum Electron. **10**, 131 (1978).
[203]V. M. Mitev, L. I. Pavlov, and K. K. Stamenov, J. Phys. B **11**, 819 (1978).
[204]M. G. Grozdeva, D. I. Metchkov, V. M. Mitev *et al.*, Opt. Commun. **23**, 77 (1977).
[205]C. Y. She and J. Reintjes, Appl. Phys. Lett. **31**, 95 (1977).
[206]J. Reintjes, L. L. Tankersley, and R. Christensen, Opt. Commun. **39**, 334 (1981).
[207]J. Reintjes, C. Y. She, R. C. Eckhardt *et al.*, Appl. Phys. Lett. **30**, 480 (1977).
[208]V. S. Ovechko and V. A. Strizhevskii, Zh. Tekh. Fiz. **52**, 144 (1982) [Sov. Phys. Tech. Phys. **27**, 98 (1982)].
[209]A. V. Aleksandrov, Kvantovaya Elektron. (Moscow) **11**, 1679 (1984) [Sov. J. Quantum Electron. **14**, 1131 (1984)].
[210]V. G. Arkhipkin, A. K. Popov, and V. P. Timofeev, Pis'ma Zh. Eksp. Teor. Fiz. **27**, 149 (1978) [JETP Lett. **27**, 137 (1978)].
[211]V. V. Krasnikov and V. S. Solomatin, Kvantovaya Elektron. (Moscow) **9**, 1251 (1982) [Sov. J. Quantum Electron. **12**, 790 (1982)].
[212]V. S. Solomatin, A. I. Meleshko, and A. V. Krasnikov, Kvantovaya Elektron. (Moscow) **6**, 1258 (1979) [Sov. J. Quantum Electron. **9**, 894 (1979)].
[213]V. G. Arkhipkin, N. P. Makarov, A. K. Popov *et al.*, Kvantovaya Elektron. (Moscow) **8**, 643 (1981) [Sov. J. Quantum Electron. **11**, 388 (1981)].
[214]S. A. Akhmanov, A. I. Val'shin, V. M. Gordienko *et al.*, Kvantovaya Elektron. (Moscow) **11**, 1897 (1984) [Sov. J. Quantum Electron. **14**, 1278 (1984)]; **13**, 1992 (1986) [**16**, 1315 (1986)].
[215]S. A. Akhmanov, V. M. Gordienko, M. S. Dzhidzhoev *et al.*, Kvantovaya Elektron. (Moscow) **13**, 1957 (1986) [Sov. J. Quantum Electron. **16**, 1291 (1986)].

[216]C. K. Rhodes, in: *Laser Techniques for Extreme Ultraviolet Spectroscopy*, eds. T. J. McIlrath and R. R. Freeman, Am. Inst. Phys., N.Y., 1982, p. 112.
[217]M. S. Dzhidzhoev, V. T. Platonenko, and A. V. Chugunov, Kvantovaya Elektron. (Moscow) **12**, 2200 (1985) [Sov. J. Quantum Electron. **15**, 1451 (1985)].
[218]V. N. Delone and V. P. Krainov, *Atoms in Strong Light Fields* (in Russian), Atomizdat, M., 1978.
[219]V. G. Arkhipkin and Yu. I. Geller, Kvantovaya Elektron. (Moscow) **10**, 1243 (1983) [Sov. J. Quantum Electron. **13**, 799 (1983)].
[220]Yu. P. Raizer, *Laser Induced Discharge Phenomena*, Consultants Bureau, N.Y., 1977. [Russ. original, Nauka, M., 1974)].
[221]V. V. Krasnikov, M. S. Pshenichnikov, and V. S. Solomatin, Pis'ma Zh. Eksp. Teor. Fiz. **43**, 115 (1986) [JETP Lett. **43**, 148 (1986)].
[222]N. B. Kornienko, Kvantovaya Elektron. (Moscow) **12**, 1592 (1985) [Sov. J. Quantum Electron. **15**, 1051 (1985)].
[223]A. K. Popov, *Introduction to Nonlinear Spectroscopy* (in Russian), Nauka, Novosibirsk, 1983.
[224]V. G. Arkhipkin, V. A. Kiyashko, A. K. Popov *et al.*, Kvantovaya Elektron. (Moscow) **7**, 181 (1980) [Sov. J. Quantum Electron. **10**, 102 (1980)].

Translated by A. Zaslavsky